BUKU PROFIL PENYELIDIKAN SKIM GERAN PENYELIDIKAN
GERAN UNIVERSITI JANGKA PENDEK / GERAN DALAM UMP

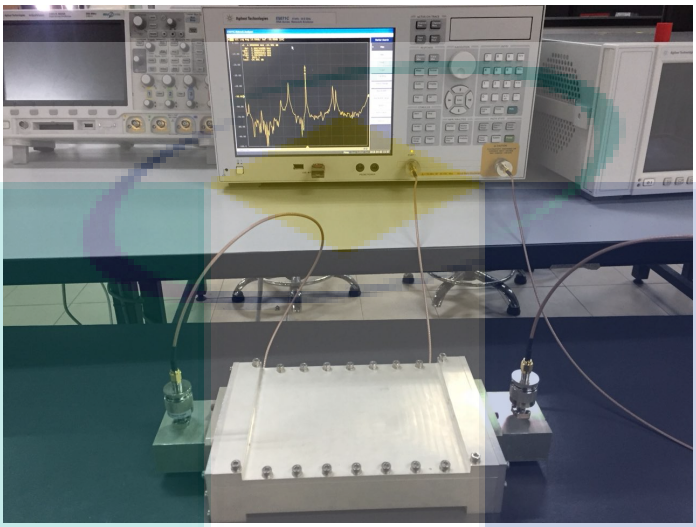

MATERIAL CHARACTERIZATION MODEL USING RECTANGULAR RESONATOR WAVEGUIDE

Mohamad Shaiful bin Abdul Karim
Ahmad Afif bin Mohd Faudzi, Nurhafizah binti Abu Talip @ Yusof, Sabira Khatun
College of Engineering
mshaiful@ump.edu.my
Microwave Engineering

ABSTRACT (120 words)

Circular cylindrical resonator has been widely used for the purpose of material characterization where the complex permittivity of the material is evaluated. However, the design of circular cylindrical resonator is not a preferable design, as it needs a precise sampling preparation so the sample fits the cavity of the resonator. Precise sample preparation is needed in order to reduce air gap between the sample and the walls of the cavity. Air gap may cause degradation of accuracy of the sample evaluation. Moreover, mostly common resonator only capable in measuring low-loss materials. The proposed rectangular resonator design is much more convenient and easy to handle, as it does not require a complex sample preparation. Samples can be in any shape or in other word, arbitrarily shape. The proposed design also has the capability in measuring low-loss and high-loss sample by varying the windows of the cavity.

1. INTRODUCTION

Material characterization has been widely used in many fields such as production of conducting textiles (Håkansson, Amiet, & Kaynak, 2007), IC packages design (Han, Li, Vieweg, Ruttan, & Polka, 2002), biosensor field (J. Kim, Babajanyan, Hovsepyan, Lee, & Friedman, 2008), food industry (Nelson, Guo, Trabelsi, & Kays, 2007) which mainly used in quality control. Material characterization is a method in determining the electrical properties of a material. In material characterization, permittivity is important in order to determine the characteristics of a material. Permittivity in simple word is the ability of a material to store electrical energy in electric field. This led to many researchers to prove their method in determining the material characterization is applicable or not. Researchers tend to compare a certain material permittivity with its relative to see whether the technique used to analyze the material is reasonable and applicable. There are many techniques used in material characterizations such as free-space method, transmission line method and resonant method. Free-space method and transmission line method categorized as non-resonant method in material characterization. Free-space method is one of the method that is applicable in material characterization. Conventional free-space measurement setup usually consists of two horn antennas and material under test (MUT). Sample is placed between the two horn antennas that act as transmitter and receiver so that it can be analyzed using Vector Network Analyzer (VNA). Commonly, free-space measurement does not need sample machining and there is no physical contact with the sample under test. It is also known as a non-destructive method in material characterization. The free-space measurement method has widely used by researcher in material characterization. (Tosaka, Fujii, Fukunaga, & Kasamatsu, 2015) developed a free-space measurement to evaluate complex relative permittivity in the range 220-330 GHz where they compared the complex relative permittivity analyzed by VNA and Time-Domain Spectroscopy (TDS). Other than free-space method, transmission line method is also one of the technique in material characterization. There are several types of transmission line – coaxial, microstrip, waveguide and stripline. (Jones, Grosvenor, & Weil, 2000) has developed a method where the insulator inside the coaxial line is replaced with the sample to be tested. S11 and S21 of the sample can be obtained from the region that filled with samples in order to characterize the material tested. (Noroozíarab, Bulja, Cahill, Kopf, & Tate, 2017) developed a method where permittivity of materials is extracted based on thin film microstrip line where the parallel plate waveguide is filled with dielectric materials to be tested. (Chung, Sertel, & Volakis, 2010) presented two methods where a tapered stripline and microstrip line are used to characterize bulk and thin materials. For the bulk materials, tapered stripline is used to characterize the samples but this method is not applicable to thin samples. Therefore, they proposed another method using microstrip line to characterize thin samples. However, the resonant method said to have a better sensitivity than the non-resonant. However, resonant method is applicable in measuring low-loss materials while the non-resonant provides high accuracy in measuring moderate-loss materials (Akhter & Akhtar, 2016). This is because the cavity of the resonator is filled with the sample and the difference in resonance frequency and Quality factor is measured (Baker-Jarvis et al., 1998). The only disadvantage of using cavity resonator is that it only applicable at narrow band and the sample to be tested need to be machined precisely (Alahnomi, Zakaria, Ruslan, & Isa, 2015).

In this project, we focused on designing a rectangular cavity resonator apart from the circular cavity resonator which commonly used in many researches. Some problems do exist when it comes to circular cylindrical cavity resonator design. One of the problem is that precise sample machining is needed when preparing the sample to be evaluated.

This is because the cavity of circular cylindrical needs to be filled by the sample precisely so there is no air gap. Air gap may cause error in the evaluation of material so it is important to make sure the sample is fitted into the cavity. Another problem is that the circular cylindrical resonator can only measure low-loss materials. There is no flexibility in the type of materials tested so it is not convenient for the measurement of lossy materials. This design tends to measure low-loss where the amplitude of S_{21} is high and high-loss material where the amplitude of S_{21} is low. This make a huge difference with other paper where the resonator can only measure either low-loss (Baker-Jarvis et al., 1998) or high-loss materials (Tameishi et al., 2014a). Other than that, the implemented design should have the ability to measure any shapes (arbitrarily shape) of materials. This can solve the problem where requirement of sample machining is no longer needed. In order to use any conventional resonator, sample machining is needed and this can alter the properties of the original materials and may affect the results.

2. RESEARCH METHODOLOGY

2.1 Formula and Mode Chart

In order to fabricate the real design of cavity resonator, it is important to define first the dimension of the cavity. There are several methods implemented in defining the dimension of the cavity. The first one is using formula:

$$f_r = \frac{1}{2\sqrt{\varepsilon\mu}}\sqrt{\left(\frac{m}{a}\right)^2 + \left(\frac{n}{b}\right)^2 + \left(\frac{p}{d}\right)^2} \quad (1)$$

where the ε is the permittivity of air and μ is the permeability of air. The equation is derived in order to create a mode chart. The x-axis and y-axis parameters of the mode chart are obtained from the derivation equation **(1)** where n is assumed as 0 since the mode chosen is $TEm0p$.

$$f = \frac{1}{2\sqrt{\varepsilon\mu}}\sqrt{\left(\frac{m}{a}\right)^2 + \left(\frac{n}{b}\right)^2 + \left(\frac{p}{d}\right)^2}$$

where $\frac{1}{\sqrt{\varepsilon\mu}} = c_0$, so rearrange the equation as:

$$(2af)^2 = c_0 m^2 + p^2 c_0 \left(\frac{a}{d}\right)^2$$

$(2af)^2$ is the y-axis and $\left(\frac{a}{d}\right)^2$ is the x-axis for the mode chart.

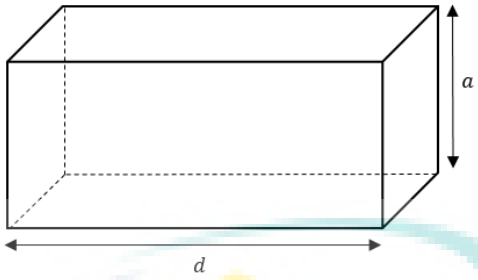

Figure 1 Dimension of cavity

The mode chosen is specifically TE_{304} where supposedly at resonant frequency, the mode is at TE_{304} should be achieved so it is possible to say that the dimension at the definite frequencies is applicable to the real-life design of the cavity. From the formula **(1)**, it is possible to derive the parameter for the mode chart. Mode chart is generated using Microsoft Excel and is reduced to show certain modes only as shown in Figure 2. In this method, a mode is chosen in order to obtain the values of a and d. The desired frequency is applied to the vertical parameter to get the value a. The ratio of the dimension a to d is chosen from the horizontal axis and the value d can be obtained by using simultaneous calculation. Mode is chosen from the uncrowded region of the graph in order to avoid overlapping with other unwanted mode. Mode TE_{304} is chosen since it is in the less crowded area at the ratio of a to d is around 0.30. If mode is chosen from the crowded region, a slight change in the dimension values will cause the mode to change to another nearest mode.

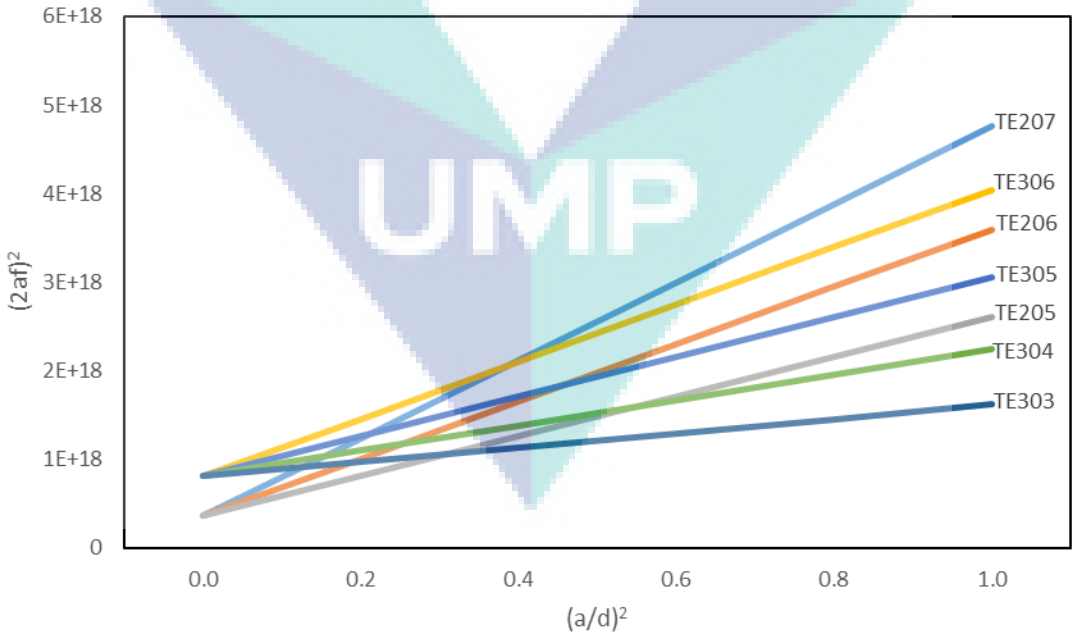

Figure 2 Mode chart

2.2 Simulation

After the mode and the resonant frequency are obtained from the mode chart and the formula of resonant frequency, the simulation in CST software is used to verify them. Obtaining the cavity's dimension only is not enough since it is impossible to fabricate a closed system in real life. In other words, there is another factor to be considered when designing a resonator that is, quality factor. In resonator method, other than resonant frequencies, quality factor is also important in determining the complex permittivity. So, external quality factor cannot be ignored completely. From the simulation, the quality factor can be calculated from the f_1, f_2 and f_c at resonant frequency with chosen mode.

In a closed system, external quality factor is known to be infinity so a small opening at the cavity can cause the external quality factor to drop to a definite large value. Quality factor will decrease significantly if the opening at the cavity is big. For small openings cavity, it possesses low amplitude of S_{21} so measuring high-loss material, the low amplitude of S_{21} will drop to become lower, possibly approaching the noise floor. This will cause inaccuracy in measurement of high-loss material so small opening is only suitable for measuring low-loss material. In this design, the opening at the center of the cavity's walls can be varied according to the type of samples tested. Since the system can measure low-loss and high-loss materials, the width of the waveguide windows must be not fixed.

In the case of measuring high-loss materials, wider window is needed since the input signal wave must be very large. High-loss materials tend to absorb energy more which eventually cause the output signal wave to be very small. Therefore, it is important to ensure the input signal wave is large enough in order to obtain readable output signal wave. So, to verify the dimension obtained from the formula and the mode chart, CST Studio Suite software is used to design the cavity resonator and to do the analysis of the scattering parameters. The operating frequency used is G-band (4 to 6 GHz).

2.2.1 Silver (AG) cavity

The simulation is run with silver (AG) cavity, which is the material that will be the real material of the cavity used in experiment. Figure 3 shows the dimension of the cavity without the waveguide. Simulation is parted into two parts that is tested with sample with various $\tan \delta$ and another part of the simulation is to assign the thickness of the cavity to $t = 22.15\ mm$ which follows the thickness of the waveguide and the sample is PTFE with various sizes is placed inside the cavity. Simulation is run with unloaded and loaded cavity to observe the resonant frequency at TE_{304}. Table 2 shows the dimension assigned for the silver cavity with 0.1 mm thickness.

Table 1 Assigned dimensions for silver cavity in CST software with t=0.1 mm

Name	Value (mm)
a	111
d	199
t	0.1
w	4 *and* 10
g	47.55
l	20

l_in	0.1
$*sample\_a$	20
$*sample\_d$	10
$*sample\_t$	0.1

* is assigned only for loaded cavity

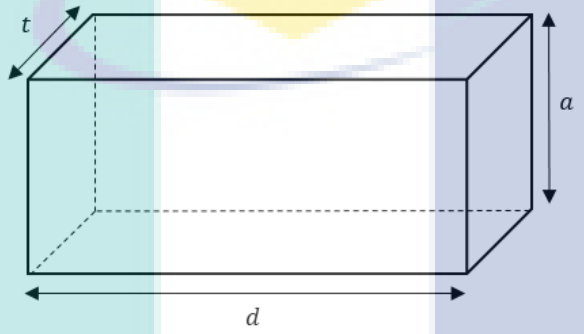

Figure 3 Dimension of cavity

The dimension of g is assigned based on the parameter of the WR-187 waveguide which has the width, $47.55\ mm$ and height, $22.15\ mm$ which equivalent to the thickness of the cavity. The dimension of l and l_in does not have any effect so there are no specific values to be assigned. But in this paper, l is assigned to $20\ mm$ and l_in to $0.1\ mm$. Figure 4 illustrates the cavity with the waveguide attached and Figure 5 shows the close up for the arm dimension that connected the waveguide and the cavity.

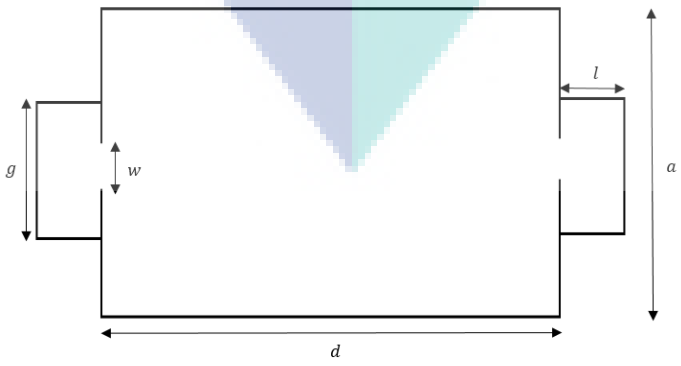

Figure 4 Dimension of cavity with waveguide attached

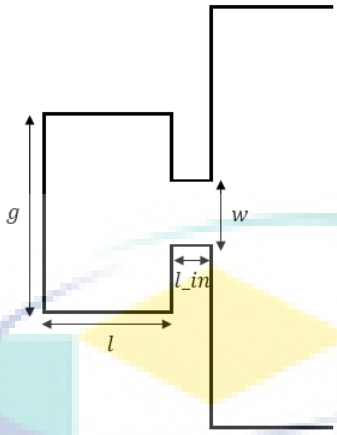

Figure 5 Close-up for the arm of the waveguide to cavity

Sample for the silver cavity is assigned to $sample\_a = 20\ mm$ and $sample\_d = 10\ mm$ while the thickness is assigned to $sample\_t = 0.1\ mm$ which is equal to the thickness of the cavity. Figure 6 illustrates the dimension of the sample used in the simulation.

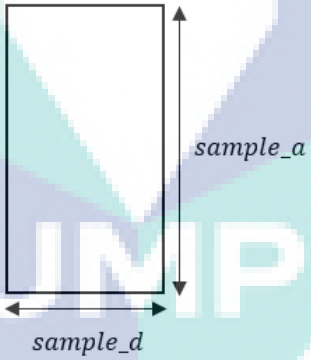

Figure 6 Dimension for the sample tested

2.2.2 Silver (AG) cavity with thickness $22.15\ mm$

At this stage of simulation, the cavity is assigned with the previous dimension as shown in Table 4 with only the thickness is different. Thickness of the cavity, t is assigned to $22.15\ mm$ in order to verify the dimension of cavity to be fabricated. The sample used in this stage is set to PTFE (Teflon) which will be used in the real measurement using the fabricated design. There are two sizes of the sample that will be tested in the simulation that is $60\ mm \times 30\ mm$ and $80\ mm \times 40\ mm$. The thickness of the sample is set to $22.15\ mm$. Table 4 shows the assigned dimension in CST software for the thickness of cavity $t = 22.15\ mm$.

Table 2 Assigned dimension for Silver cavity in CST software with t=22.15 mm

Name	Value (mm)
a	111
d	199
t	22.15
w	4 *and* 10
g	47.55
l	20
l_in	0.1
$*sample\_a$	60 *or* 80
$*sample\_d$	30 *or* 40
$*sample\_t$	22.15

* is assigned only for loaded cavity

2.3 Measurement procedure

After the verification of the dimension using CST software simulation, the dimensions are then fabricated into a practical rectangular cavity that can be used to do material characteristics measurement. The material of the cavity is silver as run in the simulation.

WR-187 waveguide at attached at both end of the cavity's openings where the range of operating frequency is from 3.95 GHz to 5.85 GHz. The waveguides are connected to the vector network analyzer (Agilent E5071C) through coaxial cable. Measurement is taken for the unloaded cavity and loaded cavity. Sample PTFE (Teflon) with different sizes are used for the measurement. Sample is placed at the center of the rectangular cavity and the amplitude of S_{21} parameters are measured using the analyser.

Before proceeding to measurement, the network analyzer should be calibrated using the calibration kit. This step is important in order to minimize any error when taking the measurement reading. After calibration has been done, the measurement can be taken.

2.4 Calibration procedure

Calibration usually takes place every time before taking the measurement. In order to calibrate the network analyzer, the coaxial cable needs to be connected to the ports of the network analyzer. Then, the coaxial cable that are connected to the ports of the network analyzer are then connected to SOLT (Short-Open-Load-Thru) to start calibration. There are five parts of calibration involving the network analyzer. One of the port from the analyzer will be connected to the "Open" port, followed by "Short" and "Load". Then both of the port are connected to each other using a connector to start the "Isolation" calibration. The last part of calibration is the isolation where each port are disconnected to each other and are isolated.

Calibrating the vector network analyzer that will be used in the measurement will remove the factors that cause measurement uncertainties which known as systematic error. Systematic error is repeatable and is non-random error, which can be removed mathematically. Any deviation from the expected results usually caused by systematic error.

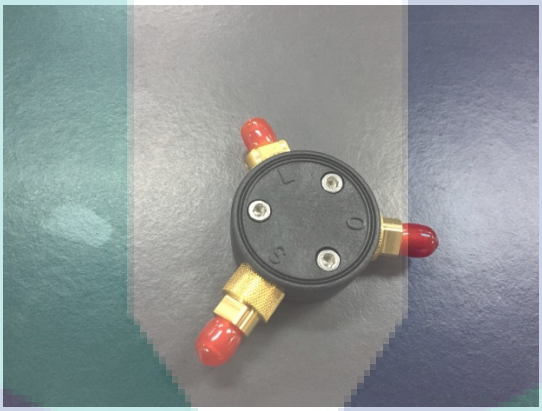

Figure 7 SOLT (SHORT-OPEN-LOAD-THRU) calibration

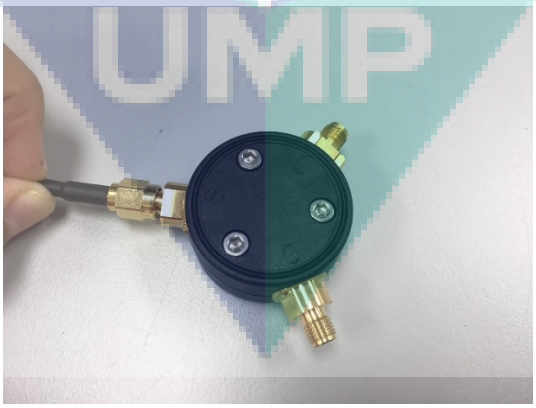

Figure 8 SOLT (SHORT-OPEN-LOAD-THRU) ports

Figure 9 Thru calibration

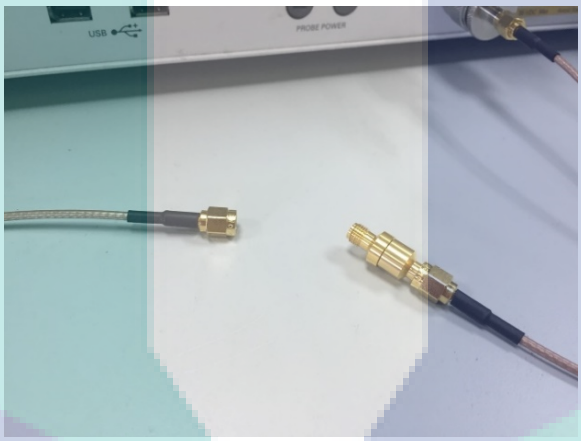

Figure 10 Isolation calibration

2.5 Measurement setup

WR-187 waveguide are attached at both end of the cavity's openings where the range of operating frequency is from 3.95 GHz to 5.85 GHz. The waveguides are connected to the vector network analyzer (Agilent E5071C) through coaxial cable. Measurement is taken for the unloaded cavity and loaded cavity. Sample PTFE (Teflon) with different sizes are used for the measurement. Sample is placed at the center of the rectangular cavity and the amplitude of S_{21} parameters are measured using the analyser. The measurement started with unloaded cavity with windows opening width equals to $4\ mm$ and followed with the measurement with windows opening width equals to $10\ mm$. The graph will be shown in the analyzer and the frequency, which TE_{304} is recorded. The range of operating frequencies are then set to 4 GHz to 6 GHz on the analyzer. The unloaded cavity with 4 mm windows' opening is the connected at the two ports of the analyzer where the amplitude of S_{21} parameter will be shown. Then the cavity is filled with samples - $60\ mm \times 30mm$ and $80\ mm \times 40\ mm$.

After the reading for 4 mm windows' openings is taken, the windows' size is changed to 10 mm and the steps are repeated as previous. Since the measurement should be taken at least three times, it should be done by batch.

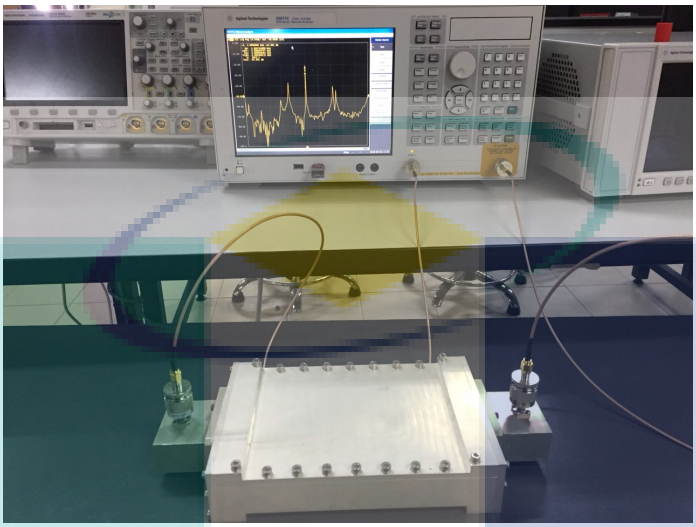

Figure 11 Measurement setup for rectangular cavity resonator to network analyser.

2.6 Method of material characterization

Material can be characterized using the prototype cavity by placing the unknown material parameter inside the cavity to be tested. The permittivity and the loss tangent of the tested material is unknown and it can be determined by using the inverse solving problem of the scattering analysis. After the simulation, the verified dimensions of the cavity are used to analyse the permittivity and loss tangent of the unknown material. In the simulation, the permittivity of the sample is pre-assigned where the resonant frequency and quality factor are then calculated. Then the permittivity is varied and the resonant frequency along with the loss tangent is calculated. From the various permittivity assigned, the minimized difference between the resonant frequency of simulation and measurement are calculated to determine the complex permittivity of the sample. Aside from determining the complex permittivity of a sample, the loss tangent should be known in order to evaluate the whole characteristics of a material. By varying the loss tangent, the minimized difference between the quality factor of the simulation and the quality factor of the measurement can be calculated. So the loss tangent of the material can be selected from the least difference from the calculation.

3. LITERATURE REVIEW

Material characterization is a technique to measure and evaluate specific characteristics of materials either from their permittivity or permeability. Permittivity is the ability of a material to store electrical energy in electric field while permeability is the measure of the ability to form a magnetic field within itself. Many methods have been associated with material characterization such as free-space method, transmission line method and resonator method.

Free-space method

Free-space method has been widely used in the application of evaluating or characterizing materials which does not destroy sample tested (Zivkovic & Murk, 2012). It is a non-destructive evaluation method that provides transmission and reflection parameters for the material characteristics (Fenner, 2015). (S. Kim, Novotny, Gordon, & Guerrieri, 2016) have developed a method to extract the complex permittivity of material where the thickness of materials tested is not taken into account. Low-loss materials such as XLPS, PTFE (Teflon) and polymethylpentene (PMP) were used as samples to be evaluated by this method. Permittivity can be obtained from S_{21} and from the real part of permittivity, the thickness of materials can be determined. Finally, the imaginary part or the loss tangent of the materials can be determined from the real part of permittivity and the thickness of samples. This method gives direct evaluation of permittivity without knowing the thickness of sample while the downside of this method is that the cost for the setup is high (goniometric stage) and the complexity of the setup and the mechanical configuration is more complex.

(Awang, Zaki, Baba, Zoolfakar, & Bakar, 2013) used a spot-focusing antenna system to measure the complex permittivity of bulk and thin film of dielectric materials at microwave frequencies. They implemented two methods – transmission method and metal-backed method. Bulk materials were evaluated using both methods while the thin film was evaluated using metal-backed method. The materials tested were Teflon-PVC, Plexiglas-PVC that are sandwiched together and for thin film, Silicon dioxide film was used. The advantage of using these method is the ability to measure the dielectric properties no matter what substrate is used at mid-range frequency. The disadvantage is that samples must be machined in the form of film because they have to be sandwiched with each other or another reference material.

Transmission line method

Transmission line on the other hand, is one of the method used in material characterization which allows simple and rapid analysis. (Han et al., 2002) demonstrated a method to characterize dielectric materials using rough surface transmission line. In this method, S_{11} and S_{12} were obtained to evaluate the complex permittivity of microstrip line. The roughness of surface was taken into account in order to prove that loss tangent can be affected from the roughness parameters. The material tested in this method was a microstrip line which is made of copper. This method is advantageous because it can be used to cut the cost of high quality and performance production of transmission line but this method also has it downside where the S_{11} parameter always cause errors in the result.

(Karim, Konishi, Harafuji, & Kitazawa, 2014) determined the complex permittivity of layered materials using waveguide measurements. This method only required the value of S_{21} in order to determine the complex permittivity of samples (individually). Materials tested were Teflon and thick microwave absorber which is made of rubber plate. The advantage of this method is that no precise machining of sample is required because the waveguide does not have to be filled until there is no air gap.

(Toda & Flaviis, 2015) developed a method to characterize substrate materials specifically at $60\ GHz$ using covered transmission line. The common two-layered stripline is modified in order to measure the permittivity up to millimeter wave (mm-wave). This method measured the permittivity of organic materials that are commonly used in low-frequency packaging such as R5880, TMM4, Ultralam, FR406 and Itera. The advantage of this method is that the variation of electrical properties of the substrate samples versus temperature is also analyzed. The downside of this method is the need to have extra precaution so that air gap can be minimized in order to reduce the effect on the accuracy of result.

Resonant method

Another method used in material characterization is by using resonant cavities. There are two types of common cavity resonators– cylindrical cavity resonator, and rectangular cavity resonator (Omar, 2011). However, there are many other alternative resonators such as ring resonator. (Zakaria et al., 2016) presented a method of material characterization by using split ring resonator (SSRR) couplings where the high sensitivity materials were evaluated. This paper proposed several designs on the couplings to affect the accuracy of the permittivity result. The materials used were simply a meat sample as they wanted to compare the coupling designs result on the evaluation of permittivity.

Cylindrical cavity resonator has been used by (Tameishi et al., 2014b) in their research to measure complex permittivity of rabbit's cornea. They used agar powder mixed with water as sample to validate their proposed method. Since cornea is high-loss and small in size, so they placed the sample at the end of the cavity resonator. Resonator commonly measure low-loss materials where the samples are placed at the center of the resonator because the electric field is at maximum. They found out that the agar sample can be measured up to $0.57\ mm$ in thickness and more than that, the sample is no longer valid in giving results since the electromagnetic waves can no longer penetrate until the end of the sample where the wall of resonator is situated. The advantage of this method is that it can measure low-loss and high-loss materials depending on to the placement of sample tested. The downside of this method is that it cannot measure that is in pure liquid form since the resonator must be kept in vertical position and meniscus may be formed which can affect the accuracy of the result.

(Saeed, Pollard, & Hunter, 2008) described a waveguide cavity resonator method to measure the complex permittivity of materials. In this method, the resonant cavity is coupled to a transmission line which result high accuracy measurements on very small volume of samples. The materials used in this method were alcohols mixed with water. This method has the ability to measure very small volume of samples indirectly provides high sensitivity and high accuracy of measurement. However, the setup is cumbersome which needs a very precise of machining on the mechanical configuration in order to make sure high sensitivity of measurement can be obtained.

(Kato & Horibe, 2016) described material characterization using resonator method by evaluating high-permittivity materials with dielectric constant up to 3,000. In this paper, two methods were implemented to evaluate the materials characteristics – sample insertion method and short circuit method. Low permittivity materials (up to several hundreds) were measured using the sample insertion method while high permittivity materials (more than 1000) were measured using short circuit method. The materials tested were majorly high permittivity materials. The disadvantage of this method is that the sample must be inserted precisely into the hole for the sample insertion method which results in only certain sample shape and size can be fitted into the hole.

(Sinha, 1967) described a design of rectangular cavity resonator where the sample tested are partially filled the cavity. This paper described a design where it can evaluate samples in the form of sheet or plane slab as many dielectric materials exist in the form of sheet. The sample partially filled the cavity of the guide either touching the side wall or at the center of the guide. The design is claimed to have simpler computational work if compared to cylindrical cavity resonator. However, there is a slight limitation to the design where the thickness of the sample is said to have a limitation in order to avoid the determination of wavelength in experiment to become more complicated. The frequencies of measurement are fixed to $8GHz$, $10\ GHz$ and $12\ GHz$. The evaluation of the real part of permittivity is obtained from the measured value of the wavelength inside the partially filled cavity. This method is said to have better accuracy and it is reliable if compared to other methods in material evaluation.

4. FINDINGS

The findings have been reported in:

1. M. S. Bin Abdul Karim, N. Binti Abu Talip Yusof and T. Kitazawa, “Scattering analysis of rectangular cavity with input and output waveguides and its application to material characterization,” 2017 IEEE Asia Pacific Microwave Conference (APMC), Kuala Lumpur, 2017, pp. 588-591.
2. S. A. Akbar, A. S. M. Shah, A. S. Abdullah, N. A. T. Yusof, S. Khatun, S. M. Shaharum, M. S. A. Karim, "An Accurate Characterization of Different Water Properties Using Resonant Method for Underwater Communication Activity", in Proceedings of the 10th National Technical Seminar on Underwater System Technology 2018, 2019, Springer Singapore, pp. 113-120.
3. S. A. Akbar, A. S. M. Shah, A. A. M. Faudzi, S. Khatun, S. M. Shaharum, N. A. T. Yusof, M. S. A. Karim, "Design of T-Shaped UWB Antenna with Dual Band Rejection Using Inverted U- and C-Shaped Slots", in Proceedings of the 10th National Technical Seminar on Underwater System Technology 2018, 2019, Springer Singapore, pp. 467-474.
4. N. Hasan, N. S. M. Hussain, N. H. S. A. Razak, N. H. Noordin, A. S. M. Shah, N. A. T. Yusof, and M. S. A. Karim, “Fabrication and Characterization of Epoxy Resin–Barium Titanate for Antenna Substrate Using Waveguide Technique”, 2020 7th International Conference on Electrical and Electronics Engineering, **under review**.
5. N. H. S. A. Razak, N. S. M. Hussain, N. H. Noordin, S. M. Shaharum, A. S. M. Shah, M. S. A. Karim “Flat Lens Design using Phase Correction Technique for Horn Antenna Applications,” International Journal of Engineering Research and Technology (IJERT), **under review**.

5. CONCLUSION

The characteristics of the material can be evaluated using the designed rectangular resonator. Teflon (PTFE) is used as the sample tested since it is a common material that being used in many researches so it is easier to compare and prove the measurement done in this paper is reliable.

The dimension of the rectangular resonator obtained in this paper is reliable since the permittivity of the Teflon tested is in the acceptable range – 2.04 to 2.09 and the loss tangent is 0.0002. There is slight difference from the measurement with the pre-measurement simulation which might due to error in the fabricated cavity's dimension. The various size of windows is used to measure low-loss and high-loss materials. This is different from the common resonator that can only measure low-loss materials. By using wider windows, high-loss materials can be measured since the loss of transmission wave is reduced. The designed cavity resonator can also measure various shape and size of material. In this paper, two sizes of PTFE are used as samples to be measured using the fabricated cavity.

In the future, this project is possible to be further to get more detailed result. Software usage is not only limited to CST but by using various software, we might cater different or more detailed result. The sizes of windows can also be varied more not only limited to 4 mm and 10 mm but wider or narrower windows can be used in taking the measurement to validate that various sizes of windows can be used in the fabricated design when taking measurement for material characterization.

This project can give benefits to the industry that requires material characterization in their production. Mobile phone production is one of the industry field that requires the determination of low-loss or high-loss materials to be used in the phone. Usually, mobile phone will use low-loss materials so that the signal loss can be minimized during its usage. Therefore, this is why material characterization is important in this industry.

ACHIEVEMENT

i) Name of articles/ manuscripts/ books published

a) M. S. Bin Abdul Karim, N. Binti Abu Talip Yusof and T. Kitazawa, "Scattering analysis of rectangular cavity with input and output waveguides and its application to material characterization," 2017 IEEE Asia Pacific Microwave Conference (APMC), Kuala Lumpur, 2017, pp. 588-591.

b) S. A. Akbar, A. S. M. Shah, A. S. Abdullah, N. A. T. Yusof, S. Khatun, S. M. Shaharum, M. S. A. Karim, "An Accurate Characterization of Different Water Properties Using Resonant Method for Underwater Communication Activity", in Proceedings of the 10th National Technical Seminar on Underwater System Technology 2018, 2019, Springer Singapore, pp. 113-120.

c) S. A. Akbar, A. S. M. Shah, A. A. M. Faudzi, S. Khatun, S. M. Shaharum, N. A. T. Yusof, M. S. A. Karim, "Design of T-Shaped UWB Antenna with Dual Band Rejection Using Inverted U- and C-Shaped Slots", in

Proceedings of the 10th National Technical Seminar on Underwater System Technology 2018, 2019, Springer Singapore, pp. 467-474.

d) N. Hasan, N. S. M. Hussain, N. H. S. A. Razak, N. H. Noordin, A. S. M. Shah, N. A. T. Yusof, and M. S. A. Karim, "Fabrication and Characterization of Epoxy Resin–Barium Titanate for Antenna Substrate Using Waveguide Technique", 2020 7th International Conference on Electrical and Electronics Engineering, **under review**.

e) N. H. S. A. Razak, N. S. M. Hussain, N. H. Noordin, S. M. Shaharum, A. S. M. Shah, M. S. A. Karim "Flat Lens Design using Phase Correction Technique for Horn Antenna Applications," International Journal of Engineering Research and Technology (IJERT), **under review**.

ii) Title of Paper presentations (international/ local)

iii) Human Capital Development

NUR SHAHIRA BINTI MAT HUSSAIN (MEG19002) – Ongoing

iv) Awards/ Others

v) Others

REFERENCES

Akhter, Z., & Akhtar, M. J. (2016). Free-Space Time Domain Position Insensitive Technique for Simultaneous Measurement of Complex Permittivity and Thickness of Lossy Dielectric Samples. *IEEE Transactions on Instrumentation and Measurement*, *65*(10), 2394–2405. https://doi.org/10.1109/TIM.2016.2581398

Alahnomi, R., Zakaria, Z., Ruslan, E., & Isa, A. (2015). Comparative Study of Materials Characterization using Microwave Resonators. *Australian Journal of Basic and Applied Sciences*, *9*, 76–85.

Awang, Z., Zaki, F. A. M., Baba, N. H., Zoolfakar, A. S., & Bakar, R. A. (2013). A Free-Space Method for Complex Permittivity Measurement of Bulk and Thin Film Dielectrics at Microwave Frequencies. *Progress In Electromagnetics Research B*, *51*, 307–328. https://doi.org/10.2528/PIERB13031509

Baker-Jarvis, J., Geyer, R. G., Grosvenor, J. H., Janezic, M. D., Jones, C. A., Riddle, B., Krupka, J. (1998). Dielectric characterization of low-loss materials a comparison of techniques. *IEEE Transactions on Dielectrics and Electrical Insulation*, *5*(4), 571–577. https://doi.org/10.1109/94.708274

Chung, J. Y., Sertel, K., & Volakis, J. L. (2010). Broadband Characterization of Bulk and Thin Magnetic Composites Using Stripline Structures. *IEEE Transactions on Microwave Theory and Techniques*, *58*(11), 2960–2967. https://doi.org/10.1109/TMTT.2010.2079050

Fenner, R. A. (2015). Analysis of free space material characterization using genetic algorithms. In *2015 IEEE International Symposium on Antennas and Propagation USNC/URSI National Radio Science Meeting* (pp. 1197–1198). https://doi.org/10.1109/APS.2015.7304987

Håkansson, E., Amiet, A., & Kaynak, A. (2007). Dielectric characterization of conducting textiles using free space transmission measurements: Accuracy and methods for improvement. *Synthetic Metals*, *157*(24), 1054–1063. https://doi.org/10.1016/j.synthmet.2007.11.001

Han, D.-H., Li, Y. L., Vieweg, R. A., Ruttan, T. G., & Polka, L. A. (2002). Dielectric material characterization using rough surface transmission lines. In *59th ARFTG Conference Digest, Spring 2002.* (pp. 4 pp.-). https://doi.org/10.1109/ARFTGS.2002.1214679

Jones, C. A., Grosvenor, J. H., & Weil, C. M. (2000). RF material characterization using a large-diameter (76.8 mm) coaxial air line. In *13th International Conference on Microwaves, Radar and Wireless Communications. MIKON - 2000. Conference Proceedings (IEEE Cat. No.00EX428)* (Vol. 2, pp. 417–420 vol.2). https://doi.org/10.1109/MIKON.2000.913959

Karim, M. S. B. A., Konishi, Y., Harafuji, K., & Kitazawa, T. (2014). Determination of Complex Permittivities of Layered Materials Using Waveguide Measurements. *IEEE Transactions on Microwave Theory and Techniques*, *62*(9), 2140–2148. https://doi.org/10.1109/TMTT.2014.2334554

Kato, Y., & Horibe, M. (2016). Permittivity measurements for high-permittivity materials at NMIJ using resonator methods. In *2016 Conference on Precision Electromagnetic Measurements (CPEM 2016)* (pp. 1–2). https://doi.org/10.1109/CPEM.2016.7540807

Kim, J., Babajanyan, A., Hovsepyan, A., Lee, K., & Friedman, B. (2008). Microwave dielectric resonator biosensor for aqueous glucose solution. *Review of Scientific Instruments*, *79*(8), 086107. https://doi.org/10.1063/1.2968115

Kim, S., Novotny, D., Gordon, J. A., & Guerrieri, J. R. (2016). A Free-Space Measurement Method for the Low-Loss Dielectric Characterization Without Prior Need for Sample Thickness Data. *IEEE Transactions on Antennas and Propagation*, *64*(9), 3869–3879. https://doi.org/10.1109/TAP.2016.2587745

Nelson, S. O., Guo, W., Trabelsi, S., & Kays, S. J. (2007). Dielectric spectroscopy of watermelons for quality sensing. *Measurement Science and Technology*, *18*(7), 1887. https://doi.org/10.1088/0957-0233/18/7/014

Norooziarab, M., Bulja, S., Cahill, R., Kopf, R., & Tate, A. (2017). Complex dielectric permittivity extraction based on multilayer thin film microstrip lines. *Antennas Propagation IET Microwaves*, *11*(7), 955–960. https://doi.org/10.1049/iet-map.2016.1045

Omar, A. (2011). *Electromagnetic Scattering and Material Characterization*. Artech House.

Saeed, K., Pollard, R. D., & Hunter, I. C. (2008). Substrate Integrated Waveguide Cavity Resonators for Complex Permittivity Characterization of Materials. *IEEE Transactions on Microwave Theory and Techniques*, *56*(10), 2340–2347. https://doi.org/10.1109/TMTT.2008.2003523

Sinha, J. K. (1967). Modified Technique for Measuring Dielectric Constants Using a Rectangular Cavity Resonator. *IEEE Transactions on Instrumentation and Measurement*, *16*(1), 32–48. https://doi.org/10.1109/TIM.1967.4313582

Tameishi, A., Kamijo, T., Suzuki, Y., Kik, A., Taki, M., & Sasaki, K. (2014a). Complex permittivity measurement method of high loss materials using cylindrical cavity resonator in millimeter-wave band. In *2014 International Symposium on Electromagnetic Compatibility, Tokyo* (pp. 541–544).

Tameishi, A., Kamijo, T., Suzuki, Y., Kik, A., Taki, M., & Sasaki, K. (2014b). Complex permittivity measurement method of high loss materials using cylindrical cavity resonator in millimeter-wave band. In *2014 International Symposium on Electromagnetic Compatibility, Tokyo* (pp. 541–544).

Toda, A. P., & Flaviis, F. D. (2015). 60-GHz Substrate Materials Characterization Using the Covered Transmission-Line Method. *IEEE Transactions on Microwave Theory and Techniques*, *63*(3), 1063–1075. https://doi.org/10.1109/TMTT.2015.2394740

Tosaka, T., Fujii, K., Fukunaga, K., & Kasamatsu, A. (2015). Development of Complex Relative Permittivity Measurement System Based on Free-Space in 220 #x2013;330-GHz Range. *IEEE Transactions on Terahertz Science and Technology*, *5*(1), 102–109. https://doi.org/10.1109/TTHZ.2014.2362013

Zakaria, Z., Alahnomi, R. A., Ruslan, E., Rashid, S. R. A., Dasril, Y., & Bahar, A. A. M. (2016). Investigation of symmetrical split ring resonator (SSRR) couplings for high sensitivity material characterization. In *2016 IEEE Asia-Pacific Conference on Applied Electromagnetics (APACE)* (pp. 122–126). https://doi.org/10.1109/APACE.2016.7915867

Zivkovic, I., & Murk, A. (2012). Free-Space Transmission Method for the Characterization of Dielectric and Magnetic Materials at Microwave Frequencies. https://doi.org/10.5772/51596

APPENDIXES

Scattering Analysis of Rectangular Cavity with Input and Output Waveguides and Its Application to Material Characterization

Mohamad Shaiful Bin Abdul Karim [#1], Nurhafizah Binti Abu Talip@Yusof [#2] and Toshihide Kitazawa [*3]
[#]*Faculty of Electric and Electronic Engineering, University of Malaysia Pahang*
26600 Pekan, Pahang, Malaysia
[1]mshaiful@ump.edu.my
[2]hafizahs@ump.edu.my
[*]*Faculty of Electric and Electronic Engineering, Ritsumeikan University*
525-8577 Shiga, Japan
[3]*kitazawa@se.ritsumei.ac.jp*

***Abstract*—A scattering analysis method is proposed to evaluate the resonant characteristics of rectangular cavity with the input and output waveguides including a columnar sample. The analytical method is based on hybrid electromagnetic procedure and affords the efficient and accurate frequency characteristics. The rectangular waveguide cavity is designed optimally by the present method, and the prototype cavity is used to evaluate the complex permittivity of the columnar samples. The virtual and actual measurements confirmed the validity of the evaluation method.**

Keywords— hybrid EM method; scattering analysis; rectangular cavity; complex permittivity

I. Introduction

An accurate evaluation of the complex permittivity of materials is important for the design of microwave devices. The resonant method has been widely used to evaluate the characteristics of low-loss materials by using a scalar network analyzer. However, most of conventional resonant methods are based on the simple theoretical methods which neglect the effect of input and output ports. This degrades the accuracy and versatility of the resonant method.

In this work, a hybrid electromagnetic method is proposed to analyze the resonant characteristics of rectangular cavity including sample with input and output waveguides. A new measurement method is proposed based on this theoretical method for evaluating dielectric characteristics of columnar sample with an arbitrarily cross-section.

II. Hybrid Electromagnetic Analysis

A columnar sample with an arbitrarily shaped cross-section is placed in a rectangular waveguide cavity as shown in Fig. 1. The sample may be a lossless or lossy dielectric material. The rectangular cavity is connected to the input and output waveguides through the windows. The dominant TE_{10} wave is incident into the cavity with the sample, and the scattered fields turned to be TE_{n0} modes are generated in the cavity. The scattered fields are analyzed by the hybrid electromagnetic method, i.e., the extended spectral domain approach (ESDA) combined with the mode-matching method, ESDMM. The analytical method is an extensions of the method reported in [1], [2], and the formulation is explained briefly in the following. The sample is divided into N thin slab layers (i) (i=1,…, N, as shown in Fig. 2), and the aperture electric fields are introduced at each interface between the layers (Fig. 3). The aperture electric fields are also introduced at the input and output windows (Fig. 3). By applying the equivalence theorem [3], each region can be treated independently.

In the homogeneous regions, the electromagnetic fields can be expressed in terms of simple sinusoidal functions in the transverse direction. In the inhomogeneous regions containing the sample, on the other hand, electromagnetic fields cannot be expressed in terms of simple sinusoidal functions. The eigen

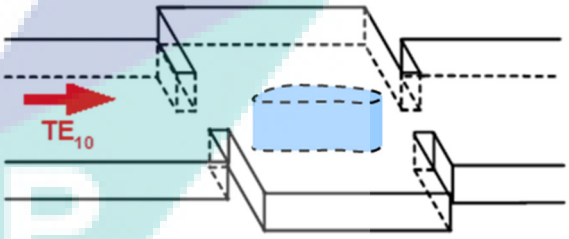

Fig. 1. Sample in arbitrary shape placed in rectangular waveguide resonator.

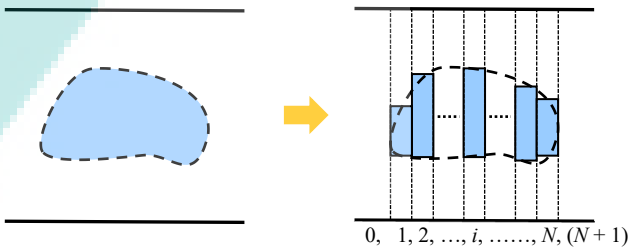

Fig. 2. Stairstep approximation.

functions, which are used to express electromagnetic fields in the inhomogeneous regions, can be constructed by using a mode-matching method [4]. These eigen functions satisfy the biorthogonal relation in the whole sample region.

By utilizing the biorthogonal relation, the electromagnetic fields in the inhomogeneous region can be transformed in spectral domain in the same way as in the homogenenous regions. In transformed domains, the Green's functions are derived easily and electromagnetic fields can be related to the aperture electric fields. The transverse magnetic fields in each region are expressed in terms of the aperture electric fields. Then, by applying the remaining continuity of the magnetic fields at the window surfaces, the integral equations on the aperture fields can be obtained. These integral equations are solved by using the Galerkin's procedure, and the aperture fields can be determined. The scattering parameters can be obtained by taking the inner product of the aperture fields with the dominant modes in the input and output waveguides.

III. Design of Rectangular Waveguide Resonator

A. Design of Rectangular Cavity

First the external dimensions of cavity are determined for the resonant mode not to be confused with other resonant modes and to have higher Q. The mode chart for the design is plotted by considering the cavity without the input and output waveguides. The proper resonant mode is selected for the material characterization. The sample material is usually placed at the center of rectangular cavity and the odd mode is preferable for measurements. The mode should be in an uncrowded region to avoid the confusion with other mode. Considering these aspects, TE_{304} mode is chosen for the measurements. Aspect ratio of the resonator (ratio of width over length) is chosen as 0.38 based on the mode chart. Then, the length of cavity is determined to get the desired value of Q.

B. Design of the Junction Between Waveguide and Cavity

The cavity is connected to the input output waveguide through the windows or irises. The narrower window is used to get higher value of external Q, which is preferable to measure low-loss samples. While the wider window is used to get larger transmitted wave, which is preferable to measure lossy samples.

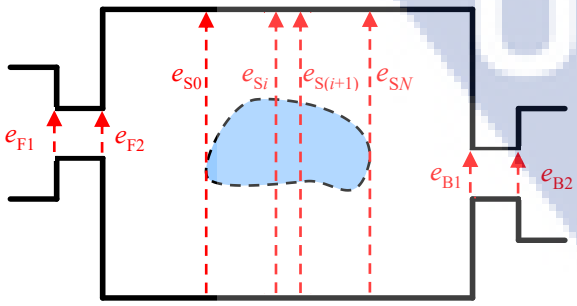

Fig. 3. Introduction of aperture electric fields.

C. Resonant characteristics of prototype cavity

Fig. 4 shows the measured frequency-dependent scattering parameters, S_{21}, of unloaded prototype cavity. The values by ESDA and finite element method (FEM) are included for comparison. The measured results are in good agreement with the values by ESDA and FEM. Especially, the measured resonant frequency for TE_{304} mode is 8.48 GHz and the same as designed.

IV. Method of Material Characterization and Virtual Experiment

The prototype cavity is used for material characterization. The unknown material parameters are estimated by solving the inverse problem of the scattering analysis based on ESDMM. A virtual experiment is performed to investigate the accuracy of the estimated complex permittivity. First, the complex permittivity of the sample is pre-assigned as $\dot{\varepsilon}_r^p$. Then, the resonant frequency, f_0 and quality factor, Q loaded with sample are calculated by FEM method. These f_0 and Q are treated as virtual measured values, whereas $\dot{\varepsilon}_r$ is unknown hereafter. Resonant frequency, f and Q are calculated by the present method (ESDMM) with varying the trial complex permittivity $\dot{\varepsilon}_r$. The most probable complex permittivity is determined by minimizing the difference between the virtual measured values and the calculated values by ESDMM method. Rectangular and T-shaped samples are used for the virtual experiment. Table I and II show values of the pre-assigned $\dot{\varepsilon}_r^p$ and the estimated $\dot{\varepsilon}_r$ for rectangular and T-shaped samples, respectively. A good reproduction was observed for both cases.

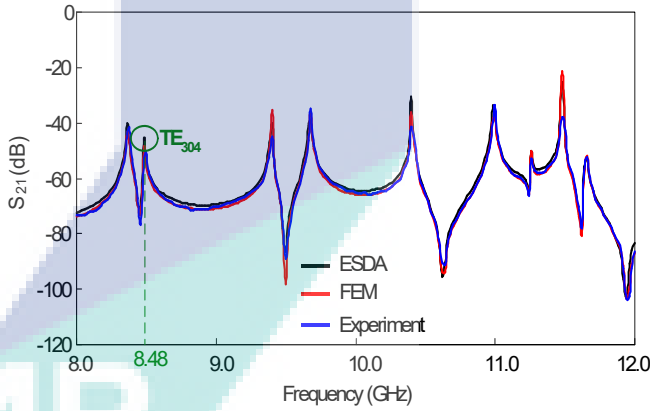

Fig. 4. Frequency-dependent scattering parameters, S_{21}, of unloaded cavity.

TABLE I. Pre-assigned and Estimated Permittivity of Rectangular Shaped Sample

Sample	Pre-assigned		Estimated	
	ε_r^p	$\tan\delta^p$	ε_r	$\tan\delta$
A	3.000	0.0100	2.990	0.0150
B	2.080	0.0004	2.077	0.0006
C	9.000	0.0100	9.040	0.0250

TABLE II. PRE-ASSIGNED AND ESTIMATED PERMITTIVITY OF T-SHAPED SAMPLE

Sample	Pre-assigned		Estimated	
	ε_r^p	tan δ^p	ε_r	tan δ
A	3.00	0.010	3.00	0.014
B	5.00	0.010	5.02	0.023
C	9.00	0.010	9.03	0.020

V. MEASUREMENT SETUP AND RESULTS

A. Measurement System

An experimental setup is assembled to measure the material characteristics in Fig. 5. X-band waveguides are used to connect with rectangular cavity and the range of operating frequency is 8.20 GHz to 12.40 GHz. Then, waveguides are connected to a network analyzer (Agilent 8719ET) through the coaxial cable. The sample is placed at the center of rectangular cavity, and the scattering parameters, $|S_{21}|$ are measured by using the network analyzer.

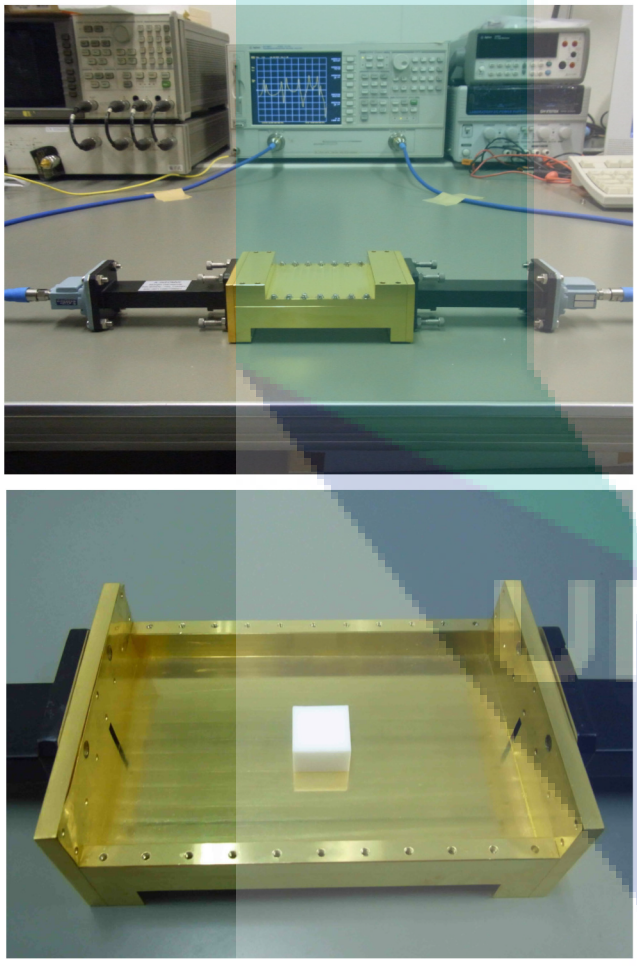

Fig. 5. Measurement setup.

B. Measurement Results

A rectangular teflon sample is prepared for the measurement. The dimension of the sample is shown in Fig. 6. Fig. 7 shows the measured frequency-dependent scattering parameters of the cavity loaded with sample. The relative permittivity, ε_r and tan δ, of the sample are evaluated by using the procedure described in section IV for TE_{304} resonant mode at 8.48 GHz. The evaluated results are shown in Table III, where the measured value obtained by the circular cavity method using TE_{011} mode [5] is included for comparison. The slight discrepancy is attributed to the air gap between cavity and waveguides caused by the deformed iris in the present measurement.

The calculated S_{21} by ESDMM and FEM using the measured ε_r and tan δ are included for comparison. The calculated results are in reasonable agreement with measured results over the operating frequencies.

TABLE III. RELATIVE PERMITIVITY ESTIMATION OF TEFLON

Method	ε_r	tan δ
Value by present method	2.039	0.00031
Value by [5]	2.039	0.00018

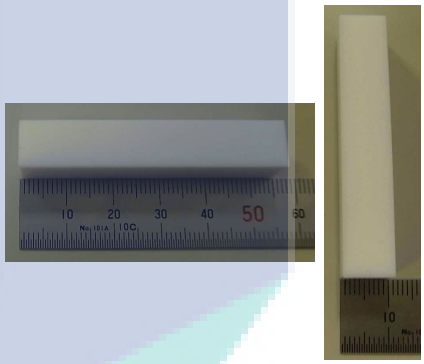

Fig. 6. Sample under test.

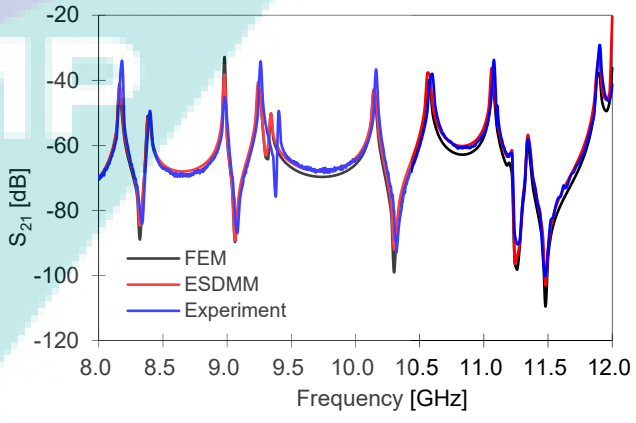

Fig. 7. Frequency-dependent scattering parameters, S_{21}.

VI. Conclusions

Scattering analytical method is presented for the rectangular cavity including sample materials with the input and output waveguides. The analytical method is based on the hybrid electromagnetic method (ESDMM) which combines the extended spectral domain approach (ESDA) with the mode-matching (MM) method and affords an efficient and accurate evaluation of the scattering parameters. The rectangular resonant cavity is designed optimally at X-band based on the method. The frequency-dependent scattering parameters $|S_{21}|$ of prototype cavity are in good agreement with the calculated values by ESDA and FEM over the frequency range between 8.2 GHz to 12.4 GHz. TE_{304} mode is used to evaluate the complex permittivity of the samples. The virtual and actual measurements confirm the validity of the evaluation method of the materials.

Acknowledgment

The work was partly supported by Research Grant RDU170370 from Research and Innovation Department, University of Malaysia Pahang.

References

[1] H. Miyagawa et al., "Simultaneous determination of complex permittivity and permeability of columnar materials with arbitrarily shaped cross-section," IEEE Trans. Microwave Theory Tech., vol. 57, pp. 2249-2256, 2009.

[2] H. Miyagawa et al., "Determination of complex permittivity and permeability of materials in rectangular waveguide using accurate hybrid numerical calculation," in Eur. Microw. Conf., Oct. 2005, vol. 1, pp. 501–504.

[3] R. F. Harrington, "Time-Harmonic Electromagnetic Fields," Piscataway, NJ: IEEE Press, 2001, ch.3, sec. 3-5, pp. 106-110.

[4] T. Shiraishi et al., "An efficient analysis of lossless and lossy discontinuities in waveguide using hybrid numerical method," IEICE Trans. Electron., vol. E86-C, no. 11, pp. 2184–2190, Nov. 2003.

[5] N. Nakao et al., "An Adaptive evaluation method of material with complex permittivity in a cylindrical cavity," International Symposium on Antennas and Propagation, Macao, pp. 1025-1028, 2010.

An Accurate Characterization of Different Water Properties Using Resonant Method for Underwater Communication Activity

Salwa Awang Akbar, Ahmad Syahiman Mohd Shah, Airul Sharizli Abdullah, Nurhafizah Abu Talip Yusof, Sabira Khatun, Syamimi Mardiah Shaharum and Mohamad Shaiful Abdul Karim

Abstract Underwater communication has a great importance in either industrial, military or for scientific purposes. The applications of underwater communication such as pollution monitoring, underwater surveillance and collection of scientific data from the bottom of the ocean require specific development of devices. In order to design these crucial devices for such activities, an accurate characteristic of water involved should be noted. The velocity of signal propagates in underwater is different from the speed of light in free space and closely related to complex permittivity. There are few types of water bodies such as rivers, streams, pond, bays, gulfs and seas where each of them possessed different characteristics. In this paper, the main focus is to determine the water bodies' characteristics by using material characterization method. This paper provides the characterization of the different water bodies such as tap water, river water, sea water and lake water where the complex permittivity are determined by using resonant method. Estimated complex permittivity of different water are in good agreement with existing method; the error is below than 6%. The present method shows a great potential to be used in characterizing wide-variety of liquid samples.

Keywords Underwater communication · Sea water · Complex permittivity Resonant method

1 Introduction

In recent year, communication devices such as mobile phone and personal computer are very essential to keep one connected with others. It is not limited only to terrestrial and satellite systems, researchers are now focusing on underwater com-

S. Awang Akbar · A. S. Mohd Shah · A. S. Abdullah · N. Abu Talip Yusof · S. Khatun
S. M. Shaharum · M. S. Abdul Karim (✉)
Faculty of Electrical and Electronics Engineering, Universiti Malaysia Pahang, 26600 Pekan, Pahang, Malaysia
e-mail: mshaiful@ump.edu.my

Z. Md Zain et al. (eds.), *Proceedings of the 10th National Technical Seminar on Underwater System Technology 2018*, Lecture Notes in Electrical Engineering 538,
https://doi.org/10.1007/978-981-13-3708-6_10

munication systems to provide the same facility for underwater environment [1]. However, the underwater communication is much more complex than the terrestrial communication due to the degradation of wave propagation velocity. In the free space, the propagation velocity of signal/wave is equal to speed of light. In other word, the effect of the permittivity can be ignored since the relative permittivity of free space is 1 and the velocity can be defined as $v = \frac{1}{\sqrt{\varepsilon_0 \mu_0}}$, where ε_0 and μ_0 are permittivity and permeability of free space, respectively. Meanwhile, factors such as salinity, temperature and density of water mainly affect the electrical property (permittivity) of the propagated medium [2], which leads to different transmission characteristics and signal propagation's behavior. The wave propagation velocity is strongly depends on permittivity, ε and permeability, μ of the propagated medium which equates as $v = \frac{1}{\sqrt{\varepsilon \mu}}$. Permeability, μ of water is same as permeability of free space. Therefore, designing underwater communication devices require an accurate characteristic (complex permittivity) of the nature involved since in our nature there are a lot of types of water bodies and each of them possessed different characteristics. It is necessary to characterize the different water bodies. The main techniques to characterize material in microwave region are free space [3], transmission-line [4–7] and resonant method [8–11].

In this paper, rectangular waveguide resonator is utilized in order to afford an accurate material characterization of the water bodies. The information of known characteristics obtained from the material characterization can be used to develop devices that are working well in underwater.

2 Method of Material Characterization

2.1 Resonant Method

Resonant method can only evaluate material at certain frequency (mono frequency), but this method is proven to be more accurate [8, 9] compared to other methods. In this paper, a rectangular waveguide resonator with adjustable size of windows, W (Fig. 1) is used in order to avoid the problems of not enough Q (quality) factor [12] and too small transmission wave. A closed system possessed a very high Q factor which approaching to infinity value. However, it is impossible to design a completely closed system so small openings in the system designed can cause the Q factor to drop to a certain value. Wide window has smaller Q factor if compared to narrower windows which means high Q factor can cause lower rate of energy loss. In order to provide high accuracy measurement of high-loss sample, large transmission signals are needed as the input to the cavity and it cannot be achieved with narrower windows. This is because narrower windows may cause the amplitude of S_{21} during measurement of high-loss materials to drop and possibly drop to the noise floor. This will cause inaccuracy in measurement readings so narrow windows are only suitable in measuring low-loss materials. Complex permittivity of sample is derived from

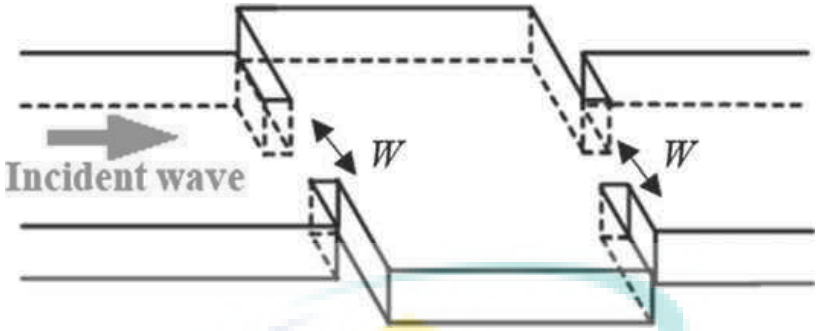

Fig. 1 Model of rectangular waveguide resonator with adjustable windows, *W*

resonant frequency and *Q* factor based on inverse problem techniques that will be explained in the next sub-chapter. *Q* factor is calculated using basic resonant circuit theory i.e. using center and −3 dB points. In measurement, resonant frequency and *Q* factor are extracted from transmission parameters, S_{21} which affected by conductor loss and external loss. In conventional resonant method, the measurement values are simply compared to simulation values that based on resonant analysis. Resonant analysis in most simulation software neglects the factor of external *Q* factor and this may lead to the degradation of measurement accuracy. Therefore, in this paper, the simulation conducted based on scattering analysis [10] and then the resonant frequency and *Q* factor are derived from the S_{21} same as measurement.

2.2 Inverse Problem

The complex permittivity for the water bodies are obtained by using the inverse solving problem. It can be done by pre-assigning the permittivity and loss of tangent values in the simulation. The difference between the simulation and the measurement will be the factors in evaluating the characteristics of the unknown material. Figure 1 shows the rectangular resonator for characterizing the samples. Input (incident wave) is fed from one side of the adjustable window and scattering parameters S_{21} of the samples will be the output.

Figure 2 shows the inverse problem technique to derive complex permittivity and loss tangent from measured resonant frequency, f and Q factor. First, the resonant frequency and Q factor are derived from the measurement (f^{mea}, Q^{mea}) and simulation (f^{sim}, Q^{sim}) results. Then, the difference of resonant frequency between measurement and simulation results are minimized by varying the value of permittivity in simulation. When the difference is below than the tolerance, the last varied value of complex permittivity is considered as best suited value for the sample. Basically the technique is also applied when deriving the value of loss tangent. In order to derive the loss tangent values from this technique, the inverse Q factor value is used. The difference between the measurement and simulation result is calculated. Then the difference

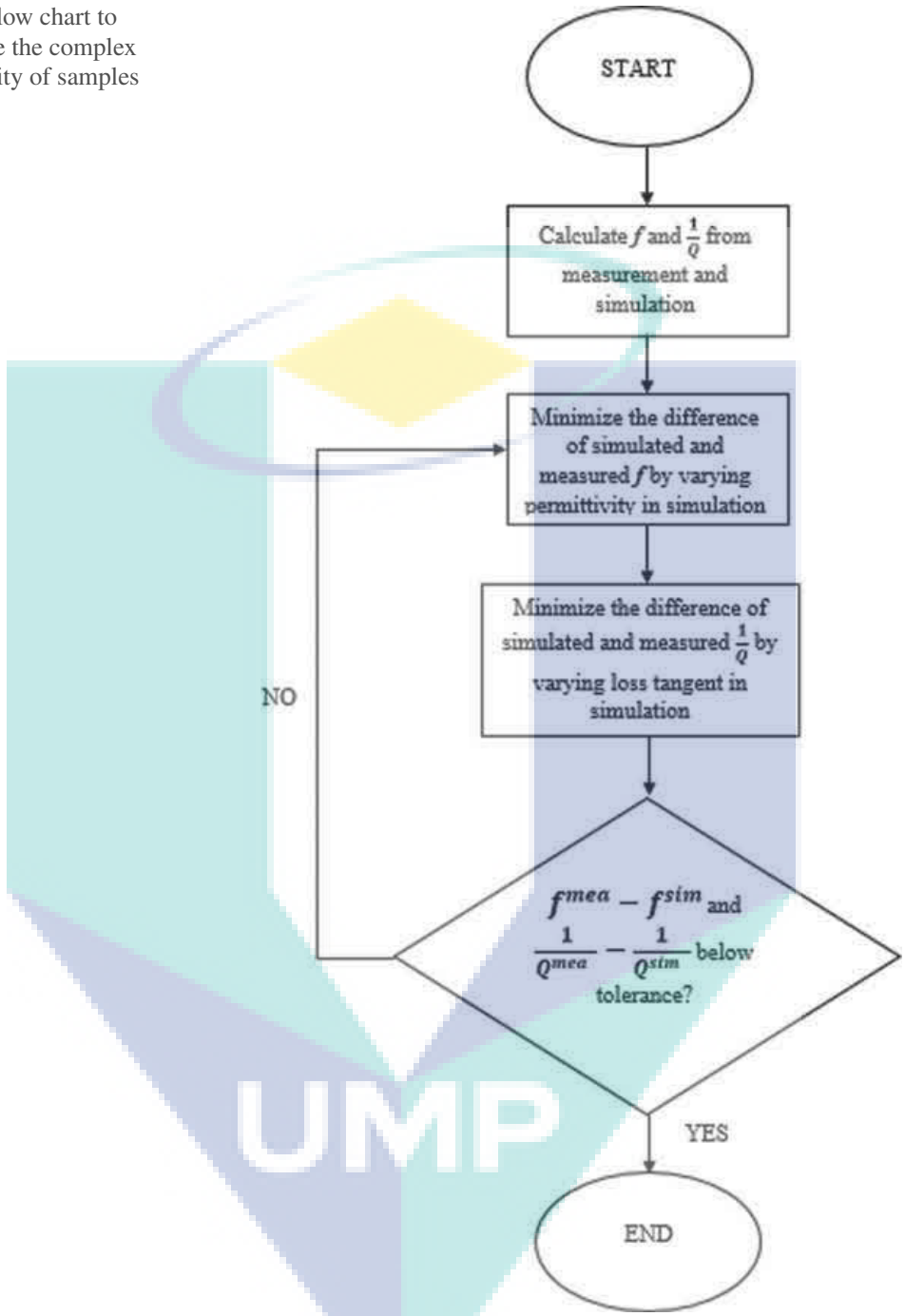

Fig. 2 Flow chart to determine the complex permittivity of samples

between measurement and simulation result is minimized by varying the value of loss tangent in simulation. When the difference is below than the tolerance, the last varied value of loss of tangent is considered as best suited value for the sample.

3 Measurement

3.1 Sample Collection and Measurement Setup

Widely-characterized samples are used in the measurement to confirm the validity of this technique, i.e., tap water and seawater available from Universiti Malaysia Pahang neighborhood. In addition, underwater communication is not only limited to an ocean and a sea environment, therefore river water and lake water are also prepared to be characterized.

Four samples of water bodies consist of tap water, river water, seawater and lake water are collected for about 500 ml each and are placed in a room temperature. The water sample is filled inside a container with the same height as resonator, inner radius 3.41 mm and outer radius 4.81 mm.

3.2 Measurement Setup

Samples are evaluated using the resonant method where a rectangular waveguide resonator is used for the material characterization and the window size used in this measurement is 10 mm which can afford −5.16 dB of transmission wave and 2651 of Q factor. Figure 3 shows the measurement setup for rectangular waveguide resonator with WR-187 waveguide connected at each end. Samples are placed at the center of the resonator using low-loss sample container and then connected to the vector network analyzer (VNA) at operating frequency from 4 to 6 GHz.

4 Results and Discussion

The parameters such as the amplitude of S_{21}, resonant frequencies and bandwidth are obtained from the measurement. The water is kept in the room temperature around 25–27 °C. After running the simulation, the results from the simulation are compared with the measurement results and the material characterization is performed as explained above. Figure 4 shows the results of the simulation and the measurement for empty cavity where both of them are compared. There is only small deviation of the resonant frequencies between the simulation and measurement so the results are fit in performing material characterization. From Fig. 4, the material characterization takes place at resonant frequency, 4.98 GHz where the mode is TE_{304} and the amplitude of S_{21} is −5.61 dB.

Table 1 shows the measured complex permittivity for all four types of water including the values from literature for comparison. The present method shows that the tap water has the highest permittivity followed by sea water, river water and lake water. Tap water also has the highest loss of tangent compared to the other three types

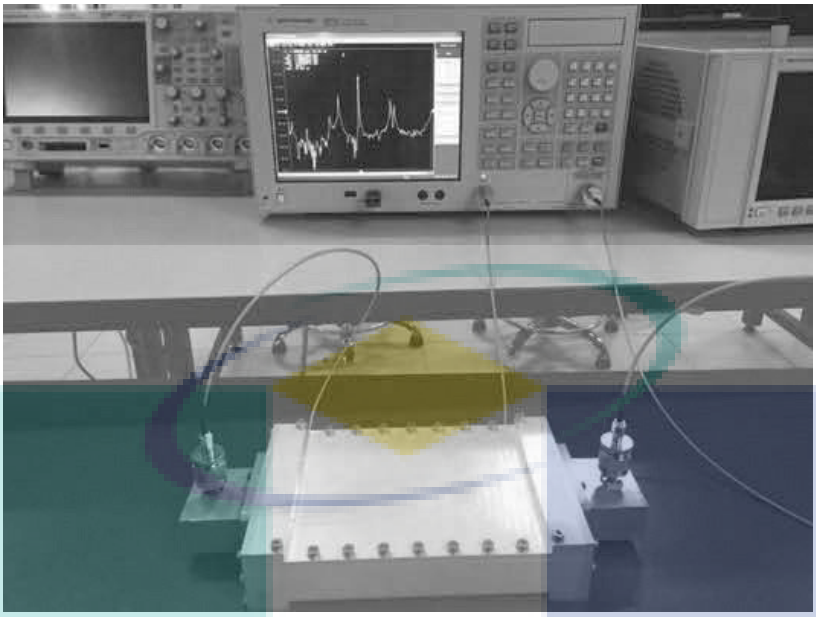

Fig. 3 Rectangular waveguide resonator with WR-187 connected to vector network analyzer

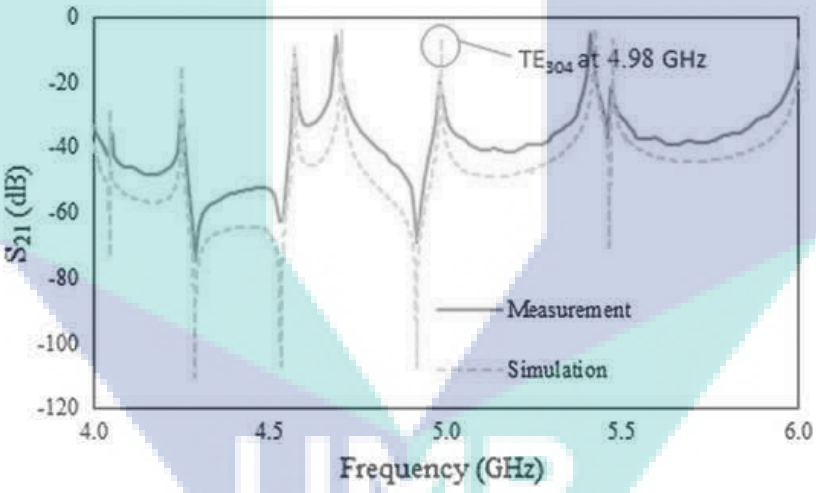

Fig. 4 Comparison between measurement and simulation result for empty cavity

of water. However, the literature value shows that the sea water has higher loss of tangent that the tap water. For tap water, the permittivity shows a good agreement with literature value [13], but not the loss tangent. This is probably because of the quality of tap water in Universiti Malaysia Pahang neighborhood is hugely affected by nearby seawater. The pH level for tap water in Universiti Malaysia Pahang neighborhood is quite higher than the normal pH level of tap water. While the permittivity and loss tangent for sea water are in the good agreement with literature [14]. The difference between permittivity and loss tangent of river water and lake water can be considered relatively small since they come from the same sources.

Table 1 Permittivity and loss of tangent for different water bodies

Sample	Present method		Literature value	
	Permittivity	Loss of tangent	Permittivity	Loss of tangent
Tap water	80.98	0.70	≈77[*1]	≈0.34[*1]
Sea water	73.89	0.42	≈78[*2]	≈0.45[*2]
River water	69.00	0.40	NA[*3]	NA[*3]
Lake water	67.02	0.30	NA[*3]	NA[*3]

[*1]Measurement had been done at 25 °C at 4 GHz [13]
[*2]Measurement had been done at 25 °C at 4 GHz and 25 ppt of salinity [14]
[*3]Complex permittivity from literature are not available

5 Conclusion

The information of the complex permittivity is very crucial to help designer to design an efficient device for underwater activity. In this paper, high loss samples of different type of waters are characterized using rectangular waveguide resonator. The model employs scattering analysis instead of resonant analysis to provide an accurate estimation of complex permittivity of samples. Measurements at G-band are done for tap water, seawater, river water and lake water. Estimated complex permittivity of seawater by present method is in good agreement with existing method and confirms the validity of the characterization technique. While the estimation of river water and lake water show that the present method has an excellent potential in determining wide-variety of liquid or water.

Acknowledgements The work was partly supported by the Research and Innovation Department, Universiti Malaysia Pahang (grant number RDU170370).

References

1. Kaushal, H., Kaddoum, G.: Underwater optical wireless communication. IEEE Access **4**, 1518–1547 (2016)
2. Zhang, X., et al.: Underwater wireless communications and networks: theory and application: Part 1 [Guest Editorial]. IEEE Commun. Mag. **53**(11), 40–41 (2015)
3. Kim, S., et al.: A free-space measurement method for the low-loss dielectric characterization without prior need for sample thickness data. IEEE Trans. Antennas Propag. **64**(9), 3869–3879 (2016)
4. Karim, M.S.B.A., Konishi, Y., Kitazawa, T.: Robustness analysis of simultaneous determination method of complex permittivity and permeability. In: 2014 international conference on numerical electromagnetic modeling and optimization for RF, microwave, and terahertz applications (NEMO), pp. 1–4, Pavia (2014)
5. Karim, M.S.B.A., et al.: Determination of complex permittivities of layered materials using waveguide measurements. IEEE Trans. Microw. Theory Tech. **62**(9), 2140–2148 (2014)

6. Kobata, T., et al.: Determination of complex permittivity of materials in rectangular waveguides using a hybrid electromagnetic method. In: Computational electromagnetics workshop (CEM), pp. 56–57, Izmir (2013)
7. Karim, M.S.B.A., Kitazawa, T.: Determination of material parameters based on hybrid numerical methods using complementary source quantities. IEICE Trans. Electron **J98-C**, 356–365 (2015)
8. Baker-Jarvis, J., et al.: Dielectric characterization of low-loss materials a comparison of techniques. IEEE Trans. Dielectr. Electr. Insul. **5**(4), 571–577 (1998)
9. Baker-Jarvis, J. et al.: Dielectric and conductor-loss characterization and measurements on electronic packaging materials. In: Technical note (NIST TN), No. 1520 (2001)
10. Karim, M.S.B.A., Binti Abu Talip Yusof, N., Kitazawa, T.: Scattering analysis of rectangular cavity with input and output waveguides and its application to material characterization. In: IEEE Asia Pacific Microwave Conference, Kuala Lumpur, pp. 588–591 (2017)
11. Kinoshita, M., et al.: A method of evaluating high-permittivity and lossy materials using a cylindrical cavity based on hybrid electromagnetic theory. Jpn. J. Appl. Phys. vol. 9, pp. 09LF03–09LF03-5 (2012)
12. Krupka, J.: Properties of shielded cylindrical quasi-TE_{0mn}-mode dielectric resonators. Trans. Microw. Theor. Tech. **36**(4), 774–779 (1988)
13. Ellison, W.J.: Permittivity of tap water, at standard atmospheric pressure, over the frequency range 0–25 T Hz and the temperature range 0–100 °C. J. Phys. Chem. Ref. Data **36**(1) (2007)
14. Somaraju, R., Trumpf, J.: Frequency, temperature and salinity variation of the permittivity of seawater. IEEE Trans. Antennas Propag. **54**(11), 3441–3448 (2006)

Design of T-Shaped UWB Antenna with Dual Band Rejection Using Inverted U- and C-Shaped Slots

Salwa Awang Akbar, Ahmad Syahiman Mohd Shah, Ahmad Afif Mohd Faudzi, Sabira Khatun, Syamimi Mardiah Shaharum, Nurhafizah Abu Talip @ Yusof and Mohamad Shaiful Abdul Karim

Abstract An ultra-wideband antenna design is proposed in this paper based on simple and easy-fabricated rectangular patch antenna. The proposed antenna is inserted with two slots; inverted U- and C-shaped to minimize interference in WiMax and WLAN band. The antenna can afford a good range of operating frequency from 2.852 to 12.176 GHz, which covers ultra-wideband frequency range set by Federal Communication Commission and in the same time be able to avoid undesired band.

Keywords U slot · C slot · UWB · Dual band · Notch frequency

1 Introduction

Ultra-wideband (UWB) antenna has been widely used in the field of military, remote sensing and radar technology [1] in these past years. UWB has a large operating bandwidth, good data transmission ratio, high resolution localization and ability to propagate through high permittivity medium even solid materials. These are the main factors lead to development UWB antenna for underwater communication. However, in this paper the design of compact antenna is proposed based on the modification of simple rectangular patch antenna to be used in free space. Different to free space, underwater environment needs consideration of conductivity, permittivity, propagation, wavelength and intrinsic impedance of water.

According to the Federal Communication Commission (FCC) on 2002, the UWB antenna frequency are covering from 3.1 to 10.6 GHz [2]. Therefore, the proposed antenna should be able to operate in these such wide frequency and in the same time, it is necessary to eliminate IEEE 802.16 WiMax and IEEE 802.11a WLAN band

S. Awang Akbar · A. S. Mohd Shah · A. A. Mohd Faudzi · S. Khatun · S. M. Shaharum
N. Abu Talip @ Yusof · M. S. Abdul Karim (✉)
Faculty of Electrical and Electronics Engineering, Universiti Malaysia Pahang,
26600 Pekan, Pahang, Malaysia
e-mail: mshaiful@ump.edu.my

Z. Md Zain et al. (eds.), *Proceedings of the 10th National Technical Seminar on Underwater System Technology 2018*, Lecture Notes in Electrical Engineering 538,
https://doi.org/10.1007/978-981-13-3708-6_40

which are allocated from 3.4 to 3.69 GHz and from 5.15 to 5.825 GHz, respectively [3]. Many researchers have proposed different shaped slots to obtain band notched frequency such as L-shaped [4], Pi-shaped [5], U-shaped [6] and C-shaped [7] slots.

In this paper, we propose a modified rectangular UWB patch antenna with a partial ground plane. Two different slots are designed to achieve Wimax and WLAN band notch characteristics. The optimization of the design is done by using electromagnetic simulation software which is based on Finite Element Method (FEM).

2 Antenna Design

2.1 Antenna Design Without Slot

The fundamental design is based on microstrip rectangular patch antenna. The dimension of the rectangular patch is 19 mm × 25 mm. Rectangular patch antenna is simple and easy to design as shown in Fig. 1a, but it cannot afford wide frequency range as mismatching impedance occurred especially at the bottom corner which leads to the power loss. Hence, in this work we utilized the step design at the edge of the rectangular to reduce the edge effect as shown Fig. 1b. Figure 1c shows the ground plane that placed at the back of the patch where only partially grounded plane is used. The antenna is designed on FR4 substrate with permittivity of 4.4. The dimension of the antenna is 25 mm × 29 mm × 1.6 mm and, the dimension of step is $W_s = 4.65$ mm and $L_s = 5.80$ mm.

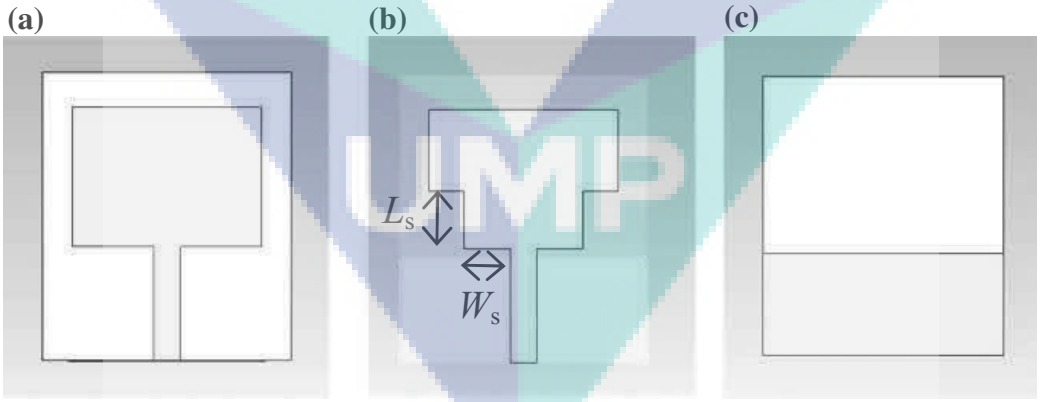

Fig. 1 Design of antenna without slot. **a** Rectangular patch antenna. **b** T-shaped patch antenna. **c** Partially ground plane

2.2 Antenna Design with Inverted U-Shaped Slot

An inverted U-shaped slot is introduced as shown in Fig. 2a to eliminate WiMax band from 3.4 to 3.69 GHz. The width and length of the slot are 0.6 and 27 mm, respectively. These dimensions are chosen mainly based on the level of difficulty during fabrication and the notched bandwidth, where the closest with WiMax band is preferable. The position of slot is very crucial as a small position error will cause the frequency shift. Therefore, in the next chapter the analysis of slot's position is presented. At first, the slot is positioned 1 mm from the top boundary between patch and substrate. Then, the distance is increased by 1 mm increment.

2.3 Antenna Design with C-Shaped Slot

While, C-shaped slot (Fig. 2b) is applied to the step design antenna in order to remove WLAN band that covers from 5.15 to 5.825 GHz. The width is fixed at 0.5 mm and length at 22 mm by considering the same aspects as explained before. Also, the position analysis of slot is conducted. The position is varied from the center of the patch until 2 mm lower than the center. The analysis starts from the center in order to avoid congestion or overlapping with the previous slot.

The analyses of inverted U- and C-shaped are conducted independently. Both slots are combined after we obtained the best dimensions and configurations, and the minor adjustment will be made.

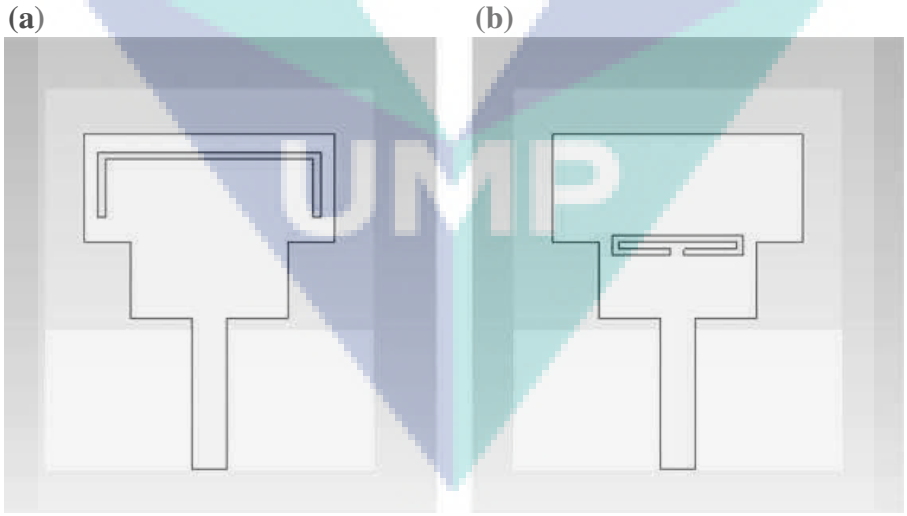

Fig. 2 An introduction of **a** inverted U-shaped slot, **b** C-shaped slot

3 Results and Discussion

3.1 Antenna Design Without Slot

Figure 3 shows the return loss of microstrip-fed T-shaped antenna. For comparison, the return loss of rectangular antenna is included. The blue region shows that the return loss is below than −10 dB and the power of antenna is radiated effectively. Because of the edge effect is reducing by introducing the step, the bandwidth is improved from only 1.668 GHz (frequency range: 3.440–5.108 GHz) to 9.372 GHz (frequency range: 3.068–12.440 GHz) which covers UWB range.

3.2 U-Shaped Slot Insertion

Figure 4 shows the comparison of return loss when the position of slot is varied. When the slot is placed near to the boundary between patch and substrate region (top), the notched frequency band is between 3.500 and 3.908 GHz, which is not removing the entire band of WiMax. For middle and bottom position, the notched band are 3.296–3.980 GHz and 2.720–4.064 GHz, respectively. Both positions are able to eliminate WiMax band but middle position is preferable since the notched band is narrower.

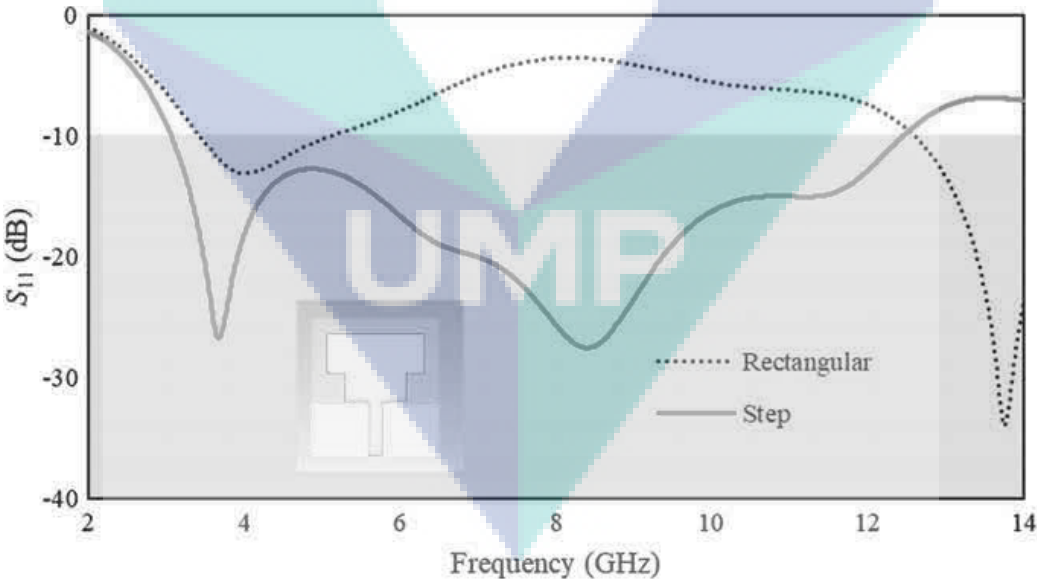

Fig. 3 Comparison of return loss for rectangular patch antenna and modified patch antenna

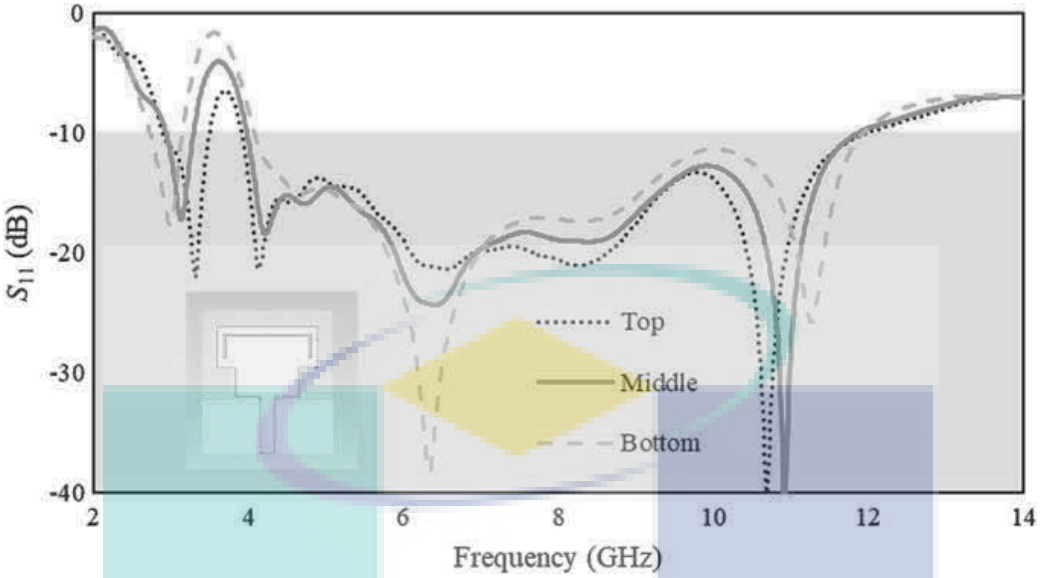

Fig. 4 Position analysis for inverted U-shaped slot

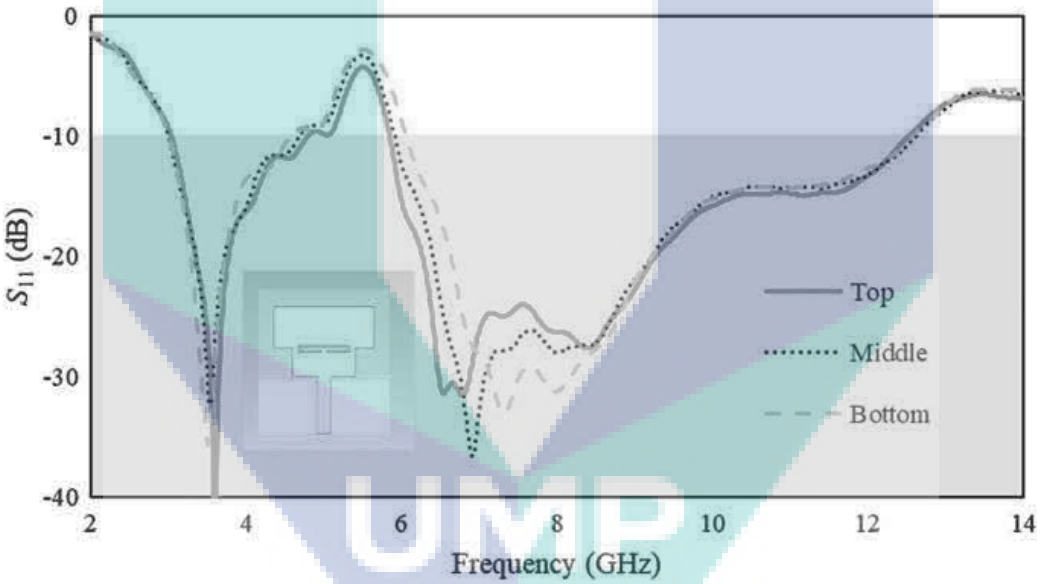

Fig. 5 Position analysis for C-shaped slot

3.3 C-Shaped Slot Insertion

Same as before, the analysis for the slot position is conducted for C-shaped slot and the result is shown in Fig. 5. The notch band is 4.808–5.840 GHz when the slot is inserted at the center of the patch (labeled as 'Top' in the graph). This position is preferable compared to lowered position where the notch band are 4.700–5.900 GHz and 4.580–6.056 GHz for middle and bottom position, respectively.

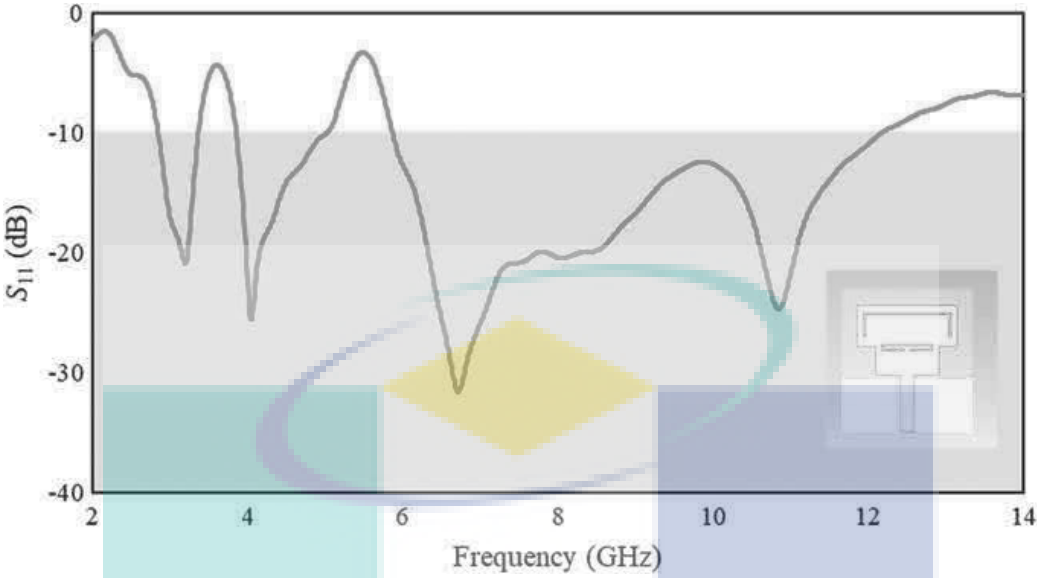

Fig. 6 Return loss of combined slots

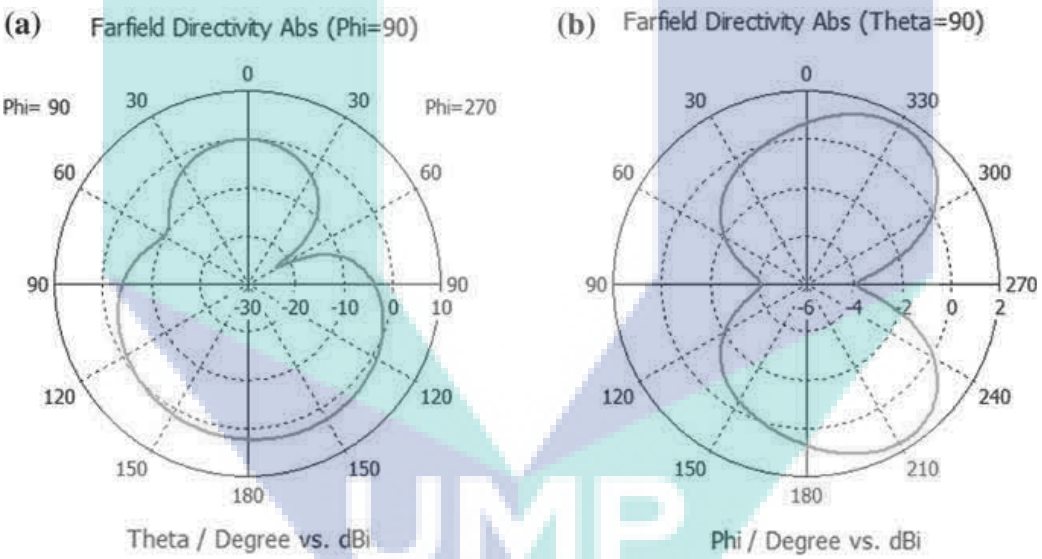

Fig. 7 Radiation pattern at 5.87 GHz in **a** E-plane and **b** H-plane

3.4 U- and C-Shaped Slot Insertion

The simulation return loss of combined slots is shown in Fig. 6. The notched frequency bands are 3.380–3.848 GHz and 5.036–5.864 GHz. In addition, the antenna can cover very wide frequency range which is between 2.852 GHz and 12.176 GHz (exceeds FCC regulations). We confirmed that the dual notch band, i.e., WiMax and WLAN can be achieved by the proposed design.

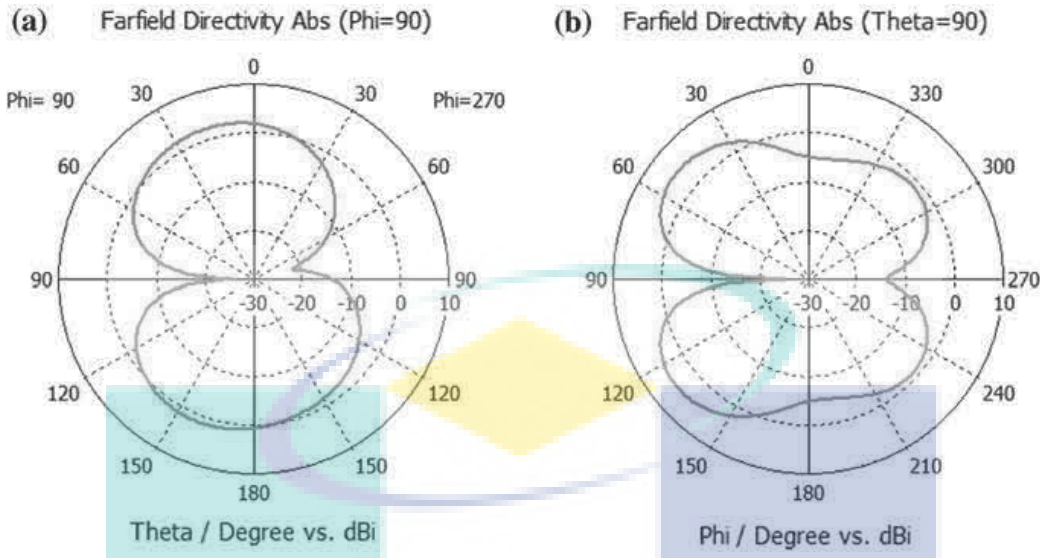

Fig. 8 Radiation pattern at 9.05 GHz in **a** E-plane and **b** H-plane

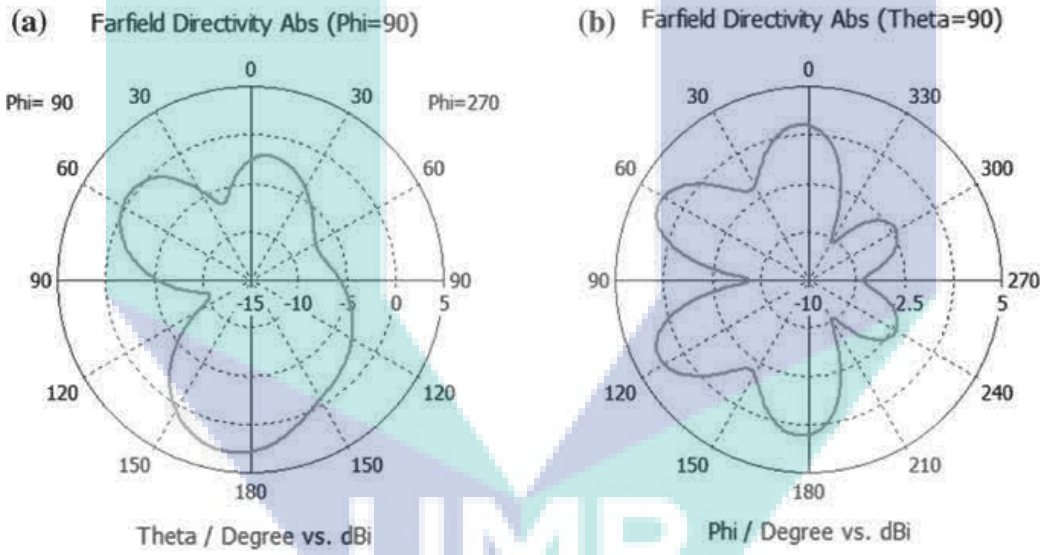

Fig. 9 Radiation pattern at 12.2 GHz in **a** E-plane and **b** H-plane

Radiation patterns for E- and H-plane at lower bound frequency 5.87 GHz, middle bound frequency 9.05 GHz and upper bound frequency 12.2 GHz are shown in Figs. 7, 8 and 9, respectively. It is observed that the radiation patterns in H-plane are in bi-directional pattern and in E-plane good radiation pattern can be obtained. Therefore, the coverage for the proposed antenna are suitable to be used in UWB application.

4 Conclusion

This work presents the design of UWB antenna using step technique for having good impedance matching. In order to avoid interference in WiMax and WLAN frequency bands, inverted U-shaped and C-shaped slots were introduced. The simulation results show that the proposed design is able to provide wide frequency range in supporting UWB systems and to eliminate the undesired bands.

Acknowledgements The work was partly supported by the Research and Innovation Department, Universiti Malaysia Pahang (grant number RDU170370). The authors would like to be grateful to the Faculty of Electrical and Electronics Engineering, Universiti Malaysia Pahang for providing financial support as well as research facilities.

References

1. Yadav, D., Tiwari, V.: UWB antenna designing: Challenges and solutions. Int. J. Comput. Commun. Instrum. Eng. **1**(1), 39–42 (2014)
2. FCC: Ultra-wideband Operation FCC Report and Order. In: Technical Report US 47 CFR Part 15 (2002)
3. Naharuddin, N.Z.A., Noordin, N.H.: Multiband UWB trapezoidal antenna using U and Pi-shaped slots. In: Electromagnetics International Workshop on Applications and Student Innovation Competition (iWEM), pp. 1–2. Hsinchu, Taiwan (2015)
4. Sam, W.Y., Zakaria, Z.: Design of a dual-notched ultra-wideband (UWB) planar antenna using L-shaped bandstop resonator. In: 11th European Conference on Antennas and Propagation (EUCAP), pp. 2237–2241. Paris (2017)
5. Antenna, P., et al.: 5 GHz WLAN band-notched UWB symmetrical slotted PI- notched parasitic planar. In: 2013 International Conference on Advances in Computing, Communications and Informatics (ICACCI), pp. 338–342. Mysore, India (2013)
6. Sudhakar, A., et al.: Single band-notched UWB square monopole antenna with double U-slot and key shaped slot. In: Fifth International Conference on Communication Systems and Network Technologies, pp. 88–92. Gwalior, India (2015)
7. Yadav, A., et al.: CSRR and C-slot loaded triple band notched ultra wideband antenna. In: International Conference on Information, Communication, Instrumentation and Control (ICICIC), pp. 1–4. Indore, India (2017)

Fabrication and Characterization of Epoxy Resin–Barium Titanate for Antenna Substrate Using Waveguide Technique

Nurulfadzilah Hasan, Nur Shahira Mat Hussain, Nur Hazimah Syazana Abdul Razak, Nurul Hazlina Noordin, Ahmad Syahiman Mohd Shah, and Mohamad Shaiful Abdul Karim
Department of Electrical Engineering
Universiti Malaysia Pahang
26300 Gambang, Pahang, Malaysia
mshaiful@ump.edu.my

Nurhafizah Abu Talip Yusof
Faculty of Electrical and Electronics Engineering Technology
Universiti Malaysia Pahang
26600 Pekan, Pahang, Malaysia
hafizahs@ump.edu.my

***Abstract*— In this paper, fabrication process of epoxy resin-barium titanate nanocomposite and measurement of its complex permittivity is presented. The material is prepared by mechanical mixing of epoxy resin and barium titanate nanopowder. The nanocomposite is intended to be used as high permittivity microstrip antenna substrate, which requires accurate measurement of its electrical characteristics. Thus, characterization of materials is done using waveguide technique, which does not require a precise machining of sample's width and thickness, and does not utilize small reflection coefficient, which can cause error in measurement. The complex permittivity of the nanocomposite is measured in G-band (4 to 6 GHz). Then, the measured values are compared with prediction method, Lichtnecker and Maxwell-Garnet method. The result shows that the measured permittivity of composite materials is in good range with prediction method, while the measurement of loss tangent shows that the developed materials is low-loss and suitable to be used as substrate of antenna.**

***Keywords- antenna substrate, barium titanate, epoxy resin, material characterization, material fabrication. Introduction* (Heading 1)**

I. INTRODUCTION

In our modern society, microwave materials have been used widely by researcher in a lot of advanced communication devices. For this reason, a wide variety of new materials have been developed especially for communication system [1], radar system [2], energy storage device [3], and industrial waste [4]. These devices require high permittivity of microwave material to develop a small, lightweight and robust design [5]. The dielectric permittivity of the composite can be enhanced by adding ferroelectric ceramics, such as barium titanate ($BaTiO_3$) and lead magnesium niobate ($MgNb_2O_9Pb_3$) [6]. They are used as fillers in dielectric composites.

In this study, a technique to prepare and characterize composite substrate of antenna, which is made of epoxy resin and barium titanate is presented. Epoxy resin has been widely used due to their low cost, high moisture, and high chemical resistance [7], while barium titanate is well known as high permittivity material [8]. Thus, the mix of these two materials can afford high value of permittivity in order to be used in compact and small antenna design.

Prediction methods such as Lichtnecker [3],[9]-[10], Maxwell-Garnett [3], [9]–[11], Jayasundere-Smith [10], effective medium theory [10], and Yamada model [9] have been used to guess the value of permittivity for composite material involving volume fraction of base matrix and ceramic material. In microwave region, the permittivity is decreasing as the frequency increases. Hence, these methods are not applicable to estimate permittivity for antenna applications, as the methods not consider frequency changes but yet important to get initial idea of permittivity during fabrication of material. In the past, many techniques have been carried out to determine complex permittivity (permittivity and loss tangent) of material in microwave measurement such as free-space method [12], resonant method [13]-[14], and transmission-line method [15]–[17]. Measurement for free-space method is among the easiest setup, which is typically, consists of two horn antennas as transmitter and receiver while the sample is placed between the antennas. However, the measurement using this method is easily affected by surrounding and cause inaccuracy determination of complex permittivity. Alternatively, resonant method able to provide high accuracy of measurement, but the measurement can be done only at one point of frequency. In this paper, the fabricated substrate is measured using transmission-line method in order to provide wide-frequency measurement while the accuracy is comparable with resonant method. G-band waveguide, frequency range from 4 to 6 GHz, is used in this method to measure scattering parameters. Then the complex permittivity will be determined from scattering parameters using an accurate and effective hybrid electromagnetic method as proposed by [18].

The rest of this paper is organized as follows. Section 2 explains the prediction of permittivity and sample fabrication of nanocomposite materials. Then, the measurement and complex permittivity estimation of fabricated materials is described in Section 3. Then, the cumulative results are presented in Section 4. Finally, Section 5 concludes our works.

II. NANOCOMPOSITE SAMPLE PREPARATION

A. Permittivity Prediction Method

In general, adding high permittivity materials such as barium titanate to a low permittivity material, such as epoxy resin will increase the permittivity of the composite. Furthermore, the permittivity increases as the concentration of filler is increase. Thus, the permittivity of a composite material can be predicted by using theoretical models such as Lichtnecker, Maxwell-Garnett, Jayasundere-Smith, effective medium theory, and Yamada model. The theoretical models relate the permittivity of the new composite material, with the permittivity and the volume fractions of base matrix and filler. In this work, commonly used Lichtnecker and Maxwell-Garnett model are adopted to verify our permittivity's measurement. The relationship between volume fraction of base matrix and ceramic material, and permittivity in Lichtnecker model [3] is given as following;

$$\ln \varepsilon_{reff} = v_1 \ln \varepsilon_{r1} + v_2 \ln \varepsilon_{r2} \quad (1)$$

where, ε_{reff} , ε_{r1} and ε_{r2} are the permittivity of the composite, base and ceramic material, respectively. v_1 and v_2 are the volume fraction of the base and ceramic material, respectively.

Meanwhile, according to Maxwell-Garnett model [3], the relationship can be represented as;

$$\frac{\varepsilon_{reff} - \varepsilon_{r2}}{\varepsilon_{reff} + 2\varepsilon_{r2}} = v_1 \frac{\varepsilon_{r1} - \varepsilon_{r2}}{\varepsilon_{r1} + 2\varepsilon_{r2}} \quad (2)$$

B. Sample Fabrication Technique

Base matrix of the composite is EpoxAmite™, epoxy resin system with medium hardener. The epoxy resin system has density of 1.25 g/cm³ and permittivity between 2.7 and 3 [5]. Filler of the composite is barium titanate nanopowder, with particle size of less than 3 µm and 98.0% purity. The density is 6 g/cm³, while the permittivity is 3279 [19].

To prepare composite material with 5 vol.% filler, first the weight ratio (wt.%) for base matrix and filler is calculated based on the filler volume ratio and density of the materials. Fabrication process starts with adding 12.63 g barium titanate nanopowder to 50 g epoxy resin system. The mixture is then stirred thoroughly using an overhead stirrer (WiseStir HS-30D) at 500 rpm for two minutes. Stirring at high speed is necessary to ensure the filler particles are well dispersed within the base matrix. However, it must be done within a short period to minimize trapped air bubbles in the mixture. Next, the mixture is placed inside a vacuum chamber (30 in.-Hg) for 2 min to remove trapped air bubbles. Then mixture is carefully poured into mold with dimension of 47.55 mm × 22.15 mm and thickness of 22.10 mm. Curing of the composite is done in two stages. First, the mixture is let to cure inside vacuum oven at 60°C for 30 minutes. This is done to remove trapped air in the mixture and improves the mechanical properties of composite [20]. The composite mixture is then further cured at room temperature for 24 hours. Finally, the cured composite is taken out of the mold and prepared for permittivity measurement. Composite preparation process is depicted in Fig. 1.

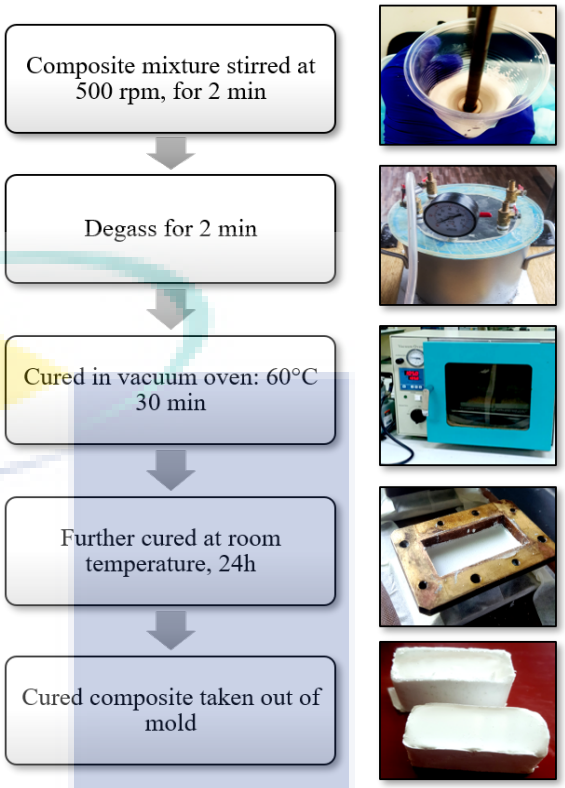

Figure 1. Material preparation process.

III. MATERIAL CHARACTERIZATION BASED ON WAVEGUIDE TECHNIQUE

A. .Sample Preparation and Measurement

Three fabricated nanocomposite samples are machined to fit the height of G-band waveguide, i.e., 22.15 mm, while the width and length can be varied in order to ease the processes of sample preparation and measurement. Fig. 2 shows the sample material under test (MUT). The dimensions for MUT 1, MUT 2 and MUT 3 are 20.94 mm × 21.96 mm, 21.12 mm × 21.77 mm, and 21.15 mm × 16.57 mm, respectively.

Fig. 3 shows the experimental setup to measure the scattering parameters. First, MUT is partially placed inside the waveguide. Then, the measurement is done by connecting the waveguide to the network analyzer using low-noise RF cable and waveguide-to-coax adapters. Partially loading MUT into the waveguide is beneficial, since TE_{10} mode characteristic; where the electric field is stronger at the center of the waveguide can be fully utilized. For instance, if the sample absorb high level of energy, the transmission parameter will

be very low and lead to inaccurate measurement. Thus, to overcome this problem, the sample might be placed at the sidewall of the waveguide where the electric field is weak so that less energy will be absorbed by the sample.

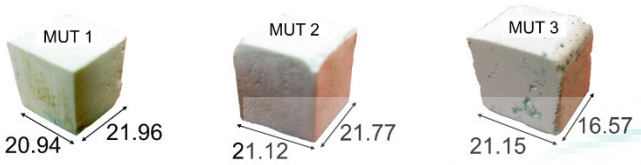

Figure 2. Material under test

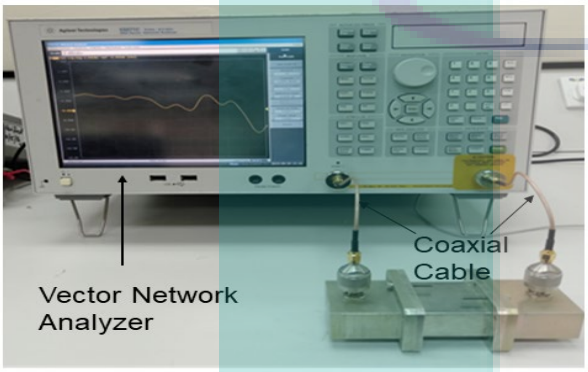

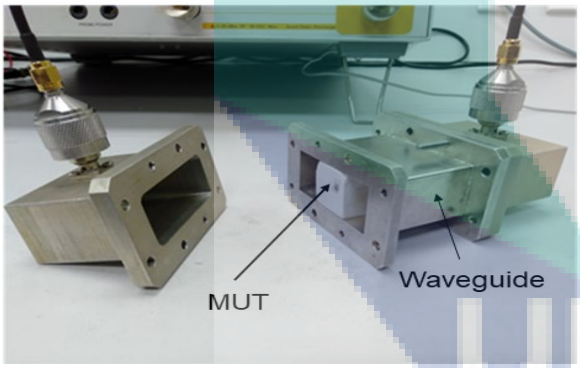

Figure 3. Measurement setup

B. *Material Characterization Technique*

To enhance the accuracy of material characterization, systematic errors is suppressed by utilizing calibration-free technique of waveguide measurement [21]. It is done by taking difference of complex transmission parameters (magnitude and phase) of waveguide measurement with and without MUT. Hence, this technique is able to eliminate electrical disturbances from measurement setup such as noise of cable and vector network analyzer (VNA).

Electrical properties in terms of complex permittivity are derived by resorting inverse technique [13] where the difference of measured and calculated complex transmission parameters are minimized by changing the complex permittivity. Once the difference is below than tolerance value, the last changed value of complex permittivity is adopted as the electrical properties of MUT. The full illustration for the material characterization technique is shown in Fig. 4.

IV. Results and Discussions

Permittivity of composite materials are measured using waveguide technique and the compared with prediction methods as mentioned above. Meanwhile, the measurement of

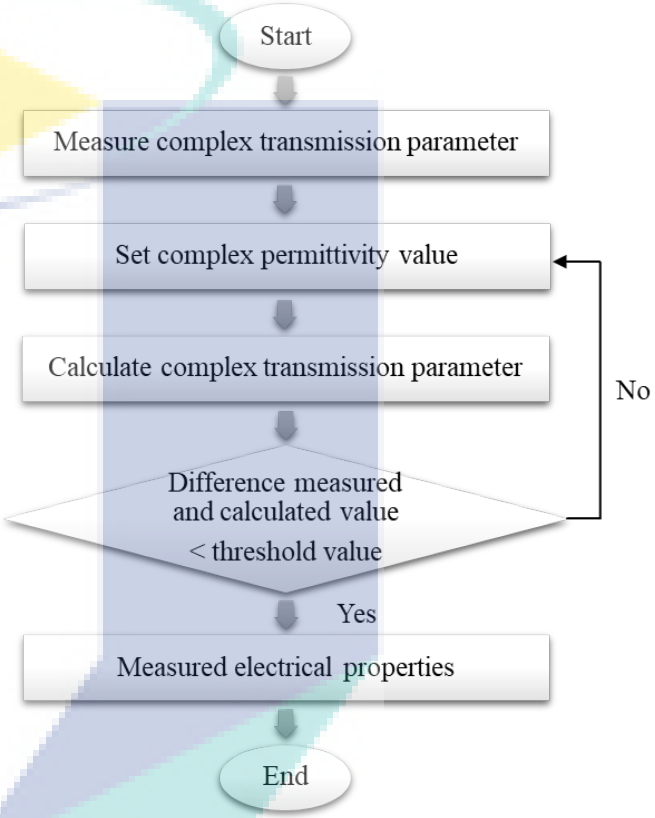

Figure 4. Material characterization flow.

loss (tangent delta) will be presented even the developed composite material is low loss, yet important for an accurate antenna design. However, there is no comparison between measurement and prediction data for tangent delta since the prediction value will lead to almost zero value due to low loss properties.

Fig. 5 shows the measured complex transmission parameters (magnitude and phase), S_{21}, for all three MUTs within frequency range of 4 to 6 GHz. There is no significant resonance of magnitude of S_{21}, so it is very promising to obtain an accurate measurement of complex permittivity. Complex permittivity is determined from complex transmission parameter by resorting the inverse technique explained above (section III).

A. *Permittivity/Dielectric Constant*

In this section, the prediction value of permittivity of epoxy resin with 5% filler of BaTiO3 is compared with the measurement value done using waveguide technique. Fig. 6

depicts the measured permittivity of all nanocomposite materials. The prediction values using Lichtnecker and Maxwell-Garnett model are included for comparison. All measured values are in good range with the predicted value. However, the measured value for each MUT is slightly different due to the difficulty to keep the same conditions during fabricating and percentage of trapped air bubbles might different. Hence, each sample has its own characteristics and measurement for each sample is necessary before using it for design purposes. It should be noted that the predicted values are not frequency-dependent. Therefore, it can be a reference for developing material but cannot be used for design purposes.

B. Tangent Delta

Value of tangent delta for these nanocomposites are small, yet important for design purposes. Fig. 7 shows the measured value of tangent delta. All three samples has tangent delta values that are consistently close to zero. Small value of tangent delta is desirable for an antenna substrate, because the loss is small.

V. CONCLUSIONS

Nanocomposite materials made of epoxy resin system as base matrix and barium titanate nanopowder as filler were fabricated for antenna applications. The necessary electrical properties for antenna designing were measured using waveguide technique at 4 to 6 GHz. This measurement method was promising since there is no resonant for measurement of scattering parameters. The measured values of permittivity were compared with two prediction methods, Lichtnecker, and Maxwell-Garnett model. They are in good range with the predicted value. Meanwhile, the measured values of loss tangent were almost zero, which is indicated that the fabricated nanocomposite material is low loss and suitable to be used as substrate of antenna.

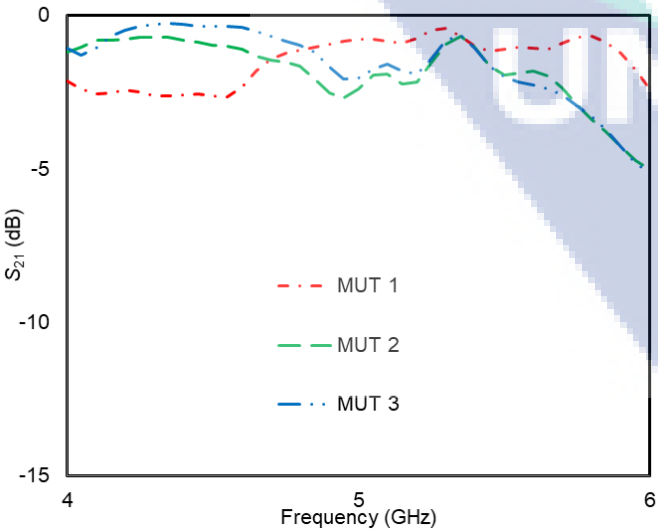

(a) Magnitude of transmission parameter, S_{21}

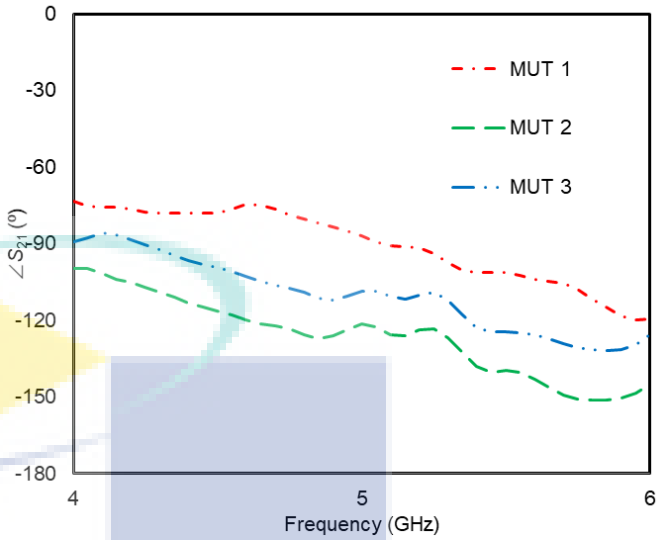

(b) Phase of transmission parameter, S_{21}

Figure 5. Measured complex transmission parameter.

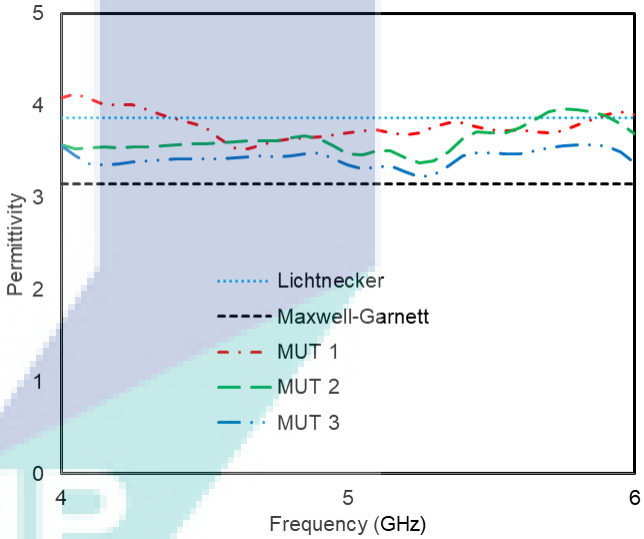

Figure 6. Comparison of measured and predicted permittivity.

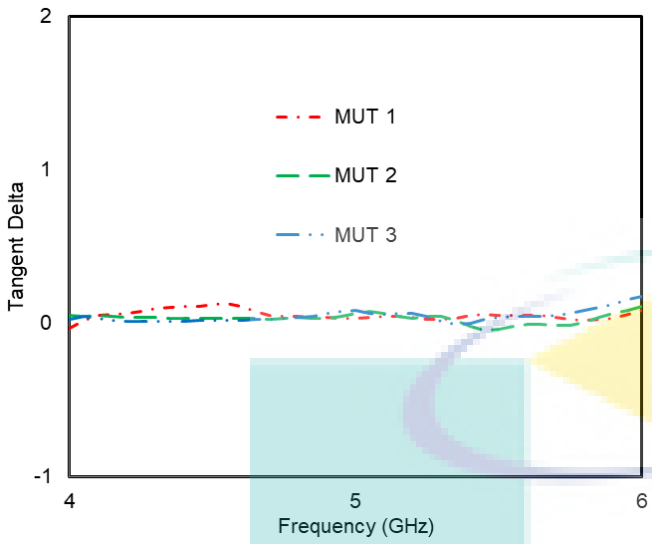

Figure 7. Measured values of tangent delta (loss tangent).

ACKNOWLEDGMENT

This work was supported in part by the Universiti Malaysia Pahang and Ministry of Education (MOE) Malaysia under Fundamental Research Grant Scheme (FRGS) with reference no. FRGS/1/2018/STG02/UMP/02/1 or RDU190140. This work also was partly supported by the Research and Innovation Department, Universiti Malaysia Pahang (grant no. RDU170370).

REFERENCES

[1] G. Peng, C. Ching, W. Chien, C. Diao, and C. Fu, "Investigation of the composites of epoxy and micro - scale BaTi4O9 ceramic powder as the substrate of microwave communication circuit," Microsyst. Technol., vol. 24, no. 1, pp. 343–349, 2018.

[2] I. L. Morrow and M. V Finnis, "Determination of the permittivity and permeability for some low-loss and high-loss microwave materials," 2016 Loughbrgh. Antennas Propag. Conf., pp. 1–4, 2016.

[3] D. S. Kim, C. Baek, H. J. Ma, and D. Kyung, "Enhanced dielectric permittivity of BaTiO3/epoxy resin composites by particle alignment," Ceram. Int., vol. 42, no. 6, pp. 7141–7147, 2016.

[4] M. S. G and A. Erdo, "Friction and wear behavior of epoxy composite filled with industrial wastes," J. Clean. Prod., vol. 237, 2019.

[5] M. S. A. Karim. N. Hasan, N. S. M. Hussain, A. A. M. Faudzi, S. M. Shaharum, N. A. T. @ Yusof, N. H. Noordin, N. A. A. Mohtadzan,, "Cured epoxy resin dielectric characterization based on accurate waveguide technique," AIP Conf. Proc. 2129, no. July, 2019.

[6] K. Cheng, C. Lin, S. Wang, S. Lin, and C. Yang, "Dielectric properties of epoxy resin – barium titanate composites at high frequency," Mater. Lett., vol. 61, pp. 757–760, 2007.

[7] P. L. Teh, M. Mariatti, H. M. Akil, C. K. Yeoh, and K. N. Seetharamu, "The properties of epoxy resin coated silica fillers composites," Mater. Lett., vol. 61, pp. 2156–2158, 2007.

[8] E. K. Nyutu, C. Chen, P. K. Dutta, and S. L. Suib, "Effect of microwave frequency on hydrothermal synthesis of nanocrystalline tetragonal barium titanate," J. Phys. Chem. C, vol. 112, no. 26, pp. 9659–9667, 2008.

[9] S. Liu, S. Xiu, B. Shen, J. Zhai, and L. B. Kong, "Dielectric properties and energy storage densities of poly(vinylidenefluoride) nanosomposite with surface hydroxylated cube shaped Ba0.6Sr0.4TiO3 nanoparticles," Polymers (Basel)., vol. 45, no. 8, pp. 10–14, 2016.

[10] B. Luo, X. Wang, Q. Zhao, and L. Li, "Synthesis , characterization and dielectric properties of surface functionalized ferroelectric ceramic / epoxy resin composites with high dielectric permittivity," Compos. Sci. Technol., vol. 112, pp. 1–7, 2015.

[11] M. H. Nisanci. F. de Paulis, A. O. Marina Y. Koledintseva and James L. Drewniak, "From maxwell garnett to debye model for electromagnetic simulation of composite dielectrics part I: random spherical inclusions," IEEE Trans. Electromagn. Compat., vol. 53, no. 4, pp. 933–942, 2011.

[12] D. K. Ghodgaonkar, V. V Varadan, and V. K. Varadan, "A free-space method for measurement of dielectric constants and loss tangents at microwave frequencies," IEEE Trans. Instrum. Meas., vol. 37, no. 8926909, 1989.

[13] S. A. Akbar, A. S. M. Shah, A. S. Abdullah, N. A. T. @ Yusof, S. Khatun, S. M. Shaharum and M. S. A. Karim, "An accurate characterization of different water properties using resonant method for underwater communication activity," Springer Nat. Singapore Pte Ltd., 2019.

[14] N. A. T. @ Yusof, M. S. A. Karim, and T. Kitazawa, "Scattering analysis of rectangular cavity with input and output waveguides and its application to material characterization," Proc. 2017 Asia Pacific Microw. Conf., pp. 5–8, 2017.

[15] A. P. Gregory and R. N. Clarke, "A review of RF and microwave techniques for dielectric measurements on polar liquids," IEEE Trans. Dielectr. Electr. Insul., vol. 13, no. 4, pp. 727–743, 2006.

[16] T. Kobata, M. Shaiful, B. Abdul, K. Momoeda, and T. Kitazawa, "Determination of complex permittivity of materials in rectangular waveguides using a hybrid electromagnetic method," CEM'13 Comput. Electromagn. Int. Work., pp. 56–57, 2013.

[17] M. Shaiful, B. Abdul, Y. Konishi, and T. Kitazawa, "Robustness analysis of simultaneous determination method of complex permittivity and permeability," 2014 Int. Conf. Numer. Electromagn. Model. Optim. RF, Microwave, Terahertz Appl., pp. 1–4, 2014.

[18] T. K. Mohamad Shaiful Bin Abd Karim, "Determination of material parameters based on hybrid numerical methods using complementary source quantities," IEICE Trans. Electron. (Japanese Ed., vol. J98-C, no. 12, pp. 356–365, 2015.

[19] B. Ertuğ, "The overview of the electrical properties of barium titanate," Am. J. Eng. Res., no. 08, pp. 1–7, 2013.

[20] D. S. Kumar, M. J. Shukla, K. K. Mahato, D. K. Rathore, R. K. Prusty, and B. C. Ray, "Effect of post-curing on thermal and mechanical behavior of GFRP composites," IOP Conf. Ser. Mater. Sci. Eng., vol. 75, no. 1, 2015.

[21] M. S. A. Karim, Y. Konishi, K. Harafuji, T. Kitazawa, and S. Member, "Determination of complex permittivities of layered materials using waveguide measurements," IEEE Trans. Microw. Theory Tech., vol. 62, no. 9, pp. 2140–2148, 2014.

Your Name	Title*	Affiliation	Research Field	Personal website
Mohamad Shaiful Abdul Karim	Senior lecturer	Universiti Malaysia Pahang	Material Characterization	http://orcid.org/0000-0001-5729-2348

Flat Lens Design using Phase Correction Technique for Horn Antenna Applications

Nur Hazimah Syazana Abdul Razak, Nur Shahira Mat Hussain, Nurul Hazlina Noordin, Syamimi Mardiah Shaharum, Ahmad Syahiman Mohd Shah, Mohamad Shaiful Abdul Karim
College of Engineering,
Universiti Malaysia Pahang,
26300 Gambang, Pahang, Malaysia
mshaiful@ump.edu.my

Nur Alia Athirah Mohtadzar
Faculty of Engineering,
Universiti Malaysia Sarawak,
94300 Kota Samarahan, Sarawak, Malaysia

***Abstract*— The design of a flat dielectric lens is presented in this study to enhance directivity of a pyramidal horn antenna. The horn antenna is proposed to cover frequency of medical imaging system, 5 to 6 GHz, and dielectric lens is designed based on phase correction techniques. The spherical waves produced by conventional horn antenna is being transform to planar waves by resorting flat lens in order to achieve a highly directive radiation in the farfield region. This is done by drilling numerous holes with different diameters through the dielectric material to produce different phase delay. The radiation characteristics of the lens are simulated using CST Microwave Studio and then compared with measured results. The results showed a good performance for radiation pattern when the lens was attached. This proposed design shows a significant increment of sidelobe level and 3-dB beamwidth between 5 and 6 GHz.**

Keywords— Horn antenna, flat lens, phase correction technique, medical imaging system, dielectric material

I. INTRODUCTION

Recently, the benefit of designing a lightweight and high directivity antenna for various applications such as horn antenna is being explored because of the actively growing number of communication systems at certain frequency. Horn antenna can provide an easy free-space measurement of microwave material [1-3], instead of complex measurement setup of waveguide [4-6] and resonator techniques [7-9]. In conventional approach, the design of high gain antenna is usually heavy and absurd long horn antenna, which is impractical. Another approach is by increasing the flare angle, but it will reduce the size of the horn antenna and will cause the horn having large quadratic phase error. The flare angle of the horn is an important factor to be considered because if it is too small, the radiated beam will not be directive. Alternatively, high gain antenna can be achieved by using lenses. Lenses are used to transform the radiation pattern of the dominant feed into some high gain radiation pattern. Lens is widely used to convert a spherical wave into planar waves for converging optical rays to a single point. The plane waves will lead to a highly directive radiation in the farfield region [10].

In previous study, two-steps and three-steps zoned dielectric lenses were designed to correct the phase of conical horn antenna at high frequency to overcome the hyperbolic lenses that is heavier and complicated in design. The stepped lenses perform best and provide comparable performance. The three-step lens response seems to be tuned high in frequency but the two-step lens is preferred as it provides nearly the same gain at both frequencies and it is uncomplicated mechanically [11]. However, the limitation of zone plate is its small operating bandwidth as compared to a lens. As the frequency is shifted away from the design frequency, the zone boundaries and thicknesses no longer satisfy the design equations, resulting in reduced focusing ability.

However, one of the dominant challenges for lens antenna is choosing the suitable materials. The lenses are often containing several different materials. These materials may not be available in commercial off-the-shelf (COTS) form [12]. Due to the lack of material demanding, it might lead to higher cost. The materials that frequently used in designing lens for a horn antenna is metamaterials. When zero refractive record metamaterials spread as a superstrate on the outside of an antenna, the radiation properties would be directive and the gain will be increases [13]. But, the fabrication processes of the metamaterials-based lenses are sometimes burdensome. In addition, metamaterials often suffer for narrow bandwidth, high losses and complicated to fabricate. It has been suggested that dielectric material could be utilized to construct an ideal lens to use in horn antenna. The dielectric lens can minimize the phase variations and also increase the directivity of the horn antenna [14]. Several low permittivity materials such as Teflon (εr = 2.1), Acrylonitrile Butadiene Styrene (ABS) (εr = 2.4) and Polyethylene (εr = 2.25) is used and the comparison shows that it offers excellent in main lobe symmetrical, small side lobe level aperture efficiency and low return loss [15-17]. Dielectric materials with low permittivity also can reduce the economic cost and the performance is satisfying [18-19].

In this paper, the lens for horn antenna is designed using low-cost and low-permittivity polylactic acid (PLA) which is positioned at the aperture of horn antenna in order to overcome the longer horn antenna. The lens is designed to be flat shape rather than hyperbolic shape for easier fabrication. The phase correction technique is utilized as it provides different phase correction at each point at the receiving part so that the waves on the transmitting side having planar wave. The lens possesses different sizes of hole where the phase of each unit cell element can be varied.

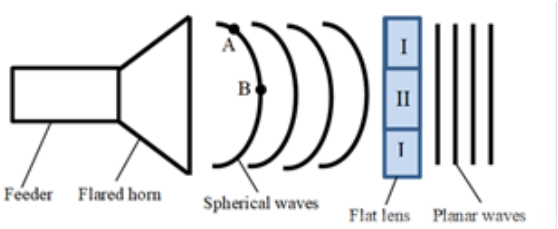

Fig. 1. Wave propagates from horn antenna through lens.

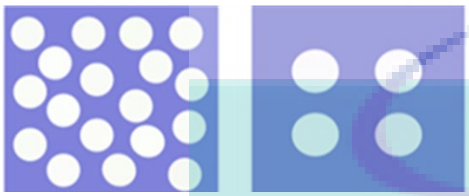

(a) (b)

Fig. 2. Varying permittivity technique: (a) increasing number of holes, (b) enlarging size of holes.

II. PHASE CORRECTION TECHNIQUE

Spherical wave propagates in unwanted outward directions that produced from the source of wave. For instance, Fig.1 shows a horn antenna with the propagated signal. The feeder of horn antenna will act as the source of wave and the spherical wave is produced due to the flare of pyramidal horn antenna where the phase is delayed at point A compared to point B. However, for some antenna applications such as biomedical imaging system [20], and through wall-imaging system [21] the planar wave is preferable instead of the spherical waves. The planar waves propagate signal into one direction so that the signal more directive compared to the spherical waves. One of the approaches to correct the signal from spherical to planar wave is phase correction technique [22]. This work utilizes the technique where, the phase at point A has to be advanced compared to the phase at point B when pass through a medium such as lens. Phase at point A can be advanced by increasing the velocity of the signal that through at region I compared the velocity at region II (refer Fig. 1). The velocity of signal propagation at each region can be varied by resorting different material. The relation between material property and velocity, v is represented by following equation;

$$v = \frac{1}{\sqrt{\varepsilon_r \mu_r}} \quad (1)$$

where, ε_r and μ_r are permittivity and permeability of medium, respectively. For dielectric material, the permeability is equal to permeability of air, μ_0. Hence, the velocity can be increased by selecting the material that has lower permittivity. There are a few approaches to increase or decrease the permittivity of a medium for example, utilizing different type of dielectric material and different thickness of material. Convex lens is one of conventional approaches that apply different thickness of material where the thickness at the center is the highest.

However, due to the complex shape of convex lens, the fabrication process becomes difficult. In this work, the flat lens is used by using only one type of dielectric material. The permittivity of the material is varied by drilling holes. Fig. 2 shows different technique to adjust the permittivity of material, which are by increasing number of holes (Fig.2 (a)) or by enlarging the size of the holes (Fig.2 (b)).

III. LENS ANTENNA DESIGN

A. Horn Antenna Design Without Lens

The fundamental design is based on pyramidal horn antenna as shown in Fig. 3. All the design is using rectangular waveguide with G-band frequency, which is between 3.95 to 5.85 GHz. The horn antenna is designed to have 15 dB of gain using WR-187 waveguide adapter as rectangular feed waveguide having dimension of 47.55×22.15 mm (a×b) and the center frequency is 5 GHz. The remaining parameters, which are a_1, b_1, ρ_e and ρ_h, are estimated using directivity formula when the directivity is optimum in E- and H-plane. The estimated parameters are shown in Table 1.

B. Horn Antenna Design With Lens

The horn antenna without lens will produce spherical waves, which are then phase-corrected by the proposed flat lens placed at the aperture of the horn. This will provide a different phase correction at each point on its receiving side so that the transmitting wave side will have the planar wave. Planar wave will result in high directive radiation in farfield region.to be defined. Do not use abbreviations in the title or heads unless they are unavoidable.

Fig. 4(a) shows the full model of proposed flat lens attached with pyramidal horn antenna, while Fig. 4(b) shows the flat lens that is design based on unit cell. The lens is constructed based on abundant of air holes having different diameter through a dielectric material. PLA with 2.72 of permittivity is chosen as the dielectric material because it is low cost and widely available in market. Before simulating the whole model, the effect of holes toward phase delay is examined by analyzing the lens in a unit cell. The structure of unit cell consists of four drilled holes and it will be analyzed by changing the diameter of hole, D. The unit cell is having two waveguide ports. The waveguide ports are set at the face of the unit cell to permit enough propagation distance and afterward the phase of the signal that is transmitted being determined. The simulation procedure is done by using CST Microwave Software. The dimensions of unit cell are given in Table 2.

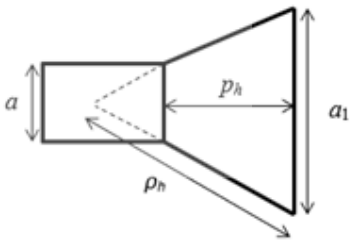

(a)

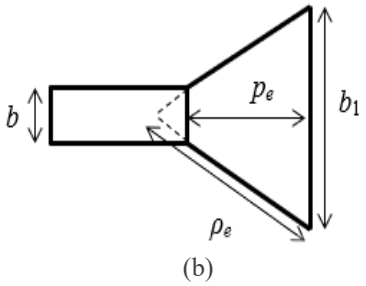

Fig. 3. Horn antenna structure for (a) H-plane and (b) E-plane view.

TABLE I. DIMENSION OF PYRAMIDAL HORN ANTENNA.

Parameter	Value (mm)
a	47.55
b	22.15
a1	154.73
b1	114.43
ρe	109.12
ρh	133.00
pe	74.94
ph	74.97

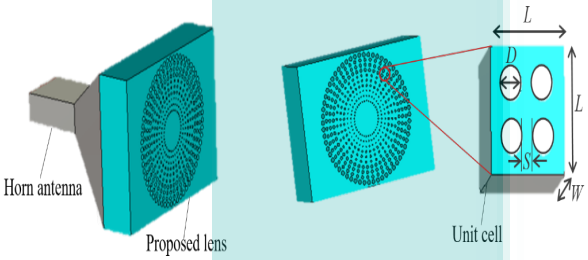

Fig. 4. (a) Full model of proposed flat lens attached with pyramidal horn antenna, (b) lens design based

IV. RESULT AND DISCUSSION

A. Phase Delay Analysis

The unit cell with varies in size of holes is simulated to examine the degrees of phase delay when a signal passed through the lens. Fig. 5 shows the phase difference when a signal passed through the hole. The diameter of the holes is varied from 0.5 to 2.0 mm in order to identify the phase that need to be corrected. The thickness of unit cell is 100 mm that is 5/3λ. The unit cell produces almost similar value with acceptable deviation as shown in Fig. 5. The transmitted signal of horn antenna will produce the difference in angle. Thus, the angle is used to correct the phase for producing the planar waves.

B. Simulation Result

The return loss, S_{11}, is simulated as shown in Fig. 6 to show the superior performance of the proposed lens. The performance is compared between the antenna with lens and without lens. As we can observed, S_{11} is within the acceptable limit, which is below the -10 dB matching line from 5 to 7 GHz for both cases. It indicates that the strength of signal received during the transmission is stable enough to obtain a good performance, i.e., more than 90% of signal transmitted through the antenna.

The simulated farfield radiation patterns are shown in Fig. 7 for selected frequency range over medical imaging system. As we can observe from the figure, the proposed lens leads to better performance of horn antenna, for instance, at 5 GHz the sidelobe level (SLL) is suppressed from -11.3 dB to -14.9 dB when the lens is attached to antenna with 3-dB beamwidth 28.5 to 14.9 degrees. This validates that the performance of the horn antenna with lens had been increased as the lobe is narrower. The narrower main lobe depicts higher intensity of radiation. It is also evident that the levels of the minor lobes and back lobes are much lower for the proposed horn antenna with lens than those without lens. The higher directivity exhibits the stronger signal radiated through the aperture of the horn antenna.

Table 3 summarizes comparison of the performance of horn antenna with and without lens which cover medical imaging system frequency range. As frequency increases, the sidelobe level (SLL) and 3-dB beamwidth show an excellent performance as it proves the directivity is also improved.

The guideline of operation of the proposed horn lens antenna is using waveguide port to launch signal from a source into horn antenna. It will create spherical wavefront like electromagnetic (EM) waves as shown in Fig. 8 (a), which are then phase-corrected by the proposed lens that is mounted at the horn aperture as shown in Fig. 8 (b). The lens will change the EM waves emanated by the horn antenna with spherical wavefront to a planar wavefront in the electric field area, and thus a high directive radiation pattern is formed.

The gain of horn antenna with and without lens is shown in Fig. 9 from 5 to 7 GHz. The gain for horn antenna with lens is higher compared to horn antenna without lens. This proves that the lens exhibits a good performance for horn antenna to improve the antenna applications.

TABLE II. LIST OF UNIT CELL SYMBOLS AND DIMENSIONS.

Symbols	Dimensions (mm)
L	30
W	35
S	(*L*-2*D*)/3

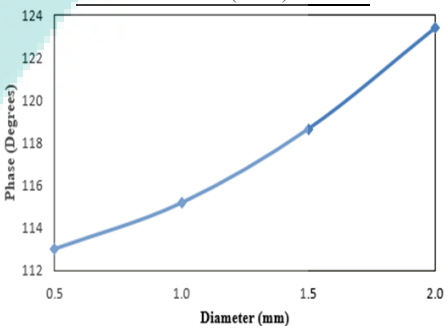

Fig. 5. Phase response at 5 GHz.

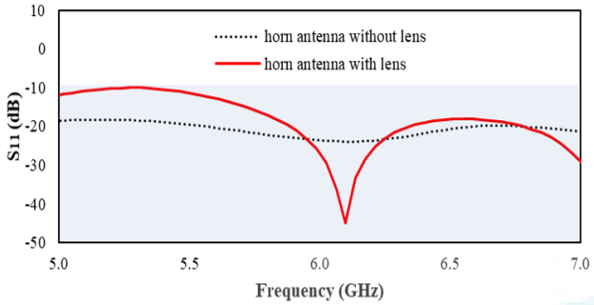

Fig. 6. Frequency dependency simulated return loss of the horn antenna.

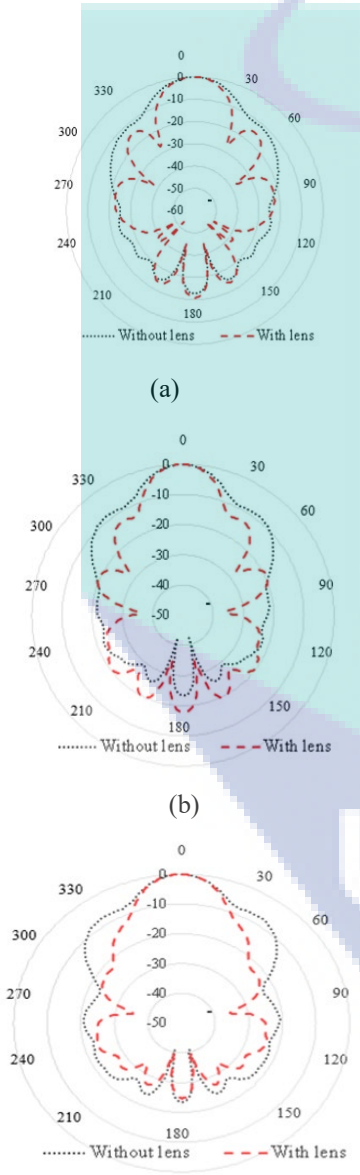

Fig. 7. The simulated far-field pattern at (a) 5 GHz, (b) 5.5 GHz and (c) 5.9 GHz.

C. *Measurement Result*

The return loss, S11, is measured using Vector Network Analyzer (VNA) as shown in Fig. 10. The performance is compared between the horn antenna with lens and without lens after being fabricated using 3D printer machine. The return loss, S11 for the antenna without lens is below than -10 dB from 5 to 7 GHz. Based on these performances, the antenna with lens still can be used for medical imaging system because the frequency range for medical imaging system in Malaysia is from 5 to 6 GHz.

The measured farfield radiation patterns are shown in Fig. 11 for 5 GHz, 5.5 GHz and 5.9 GHz. Please be noted that the value of gain does not represent the real values since the measurement had been done by using vector network analyzer instead of signal generator and spectrum analyzer. Across the frequency range for biomedical imaging, the sidelobe level is below than -3 dB for the antenna with lens, where the sidelobe level is suppressed. While, the 3-dB beamwidth become narrower compared to those without lens at observed frequencies. The summary of the measured values of SLL and beamwidth of horn antenna with and without lens are shown in Table 4.

However, if we compare the performance of return loss, SLL and 3-dB beamwidth between the simulated and measured results, the fabricated antenna shows the degradation of the performance. The main factor of this discrepancy is the imperfection during fabrication because of our 3D printer machine limitations. The limitations involve the low density of printing infill, poor accuracy of fabrication, and unsmooth printing surface.

TABLE III. THE SIMULATED RADIATION CHARACTERISTIC OF THE HORN ANTENNA WITH AND WITHOUT LENS.

Frequency (GHz)	SLL (dB)		3-dB Beamwidth (Degrees)	
	Without lens	With lens	Without lens	With lens
5.0	-11.3	-14.9	28.5	14.9
5.5	-8.6	-13.0	25.5	21.6
5.9	-7.4	-22.3	24.2	22.5

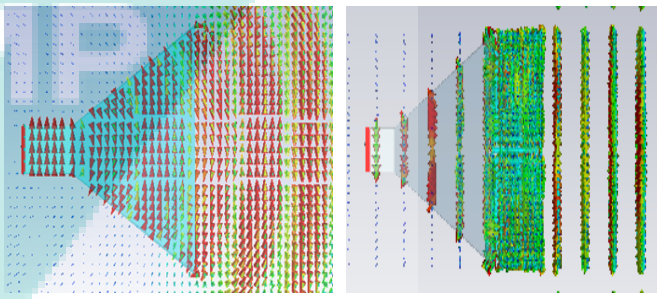

Fig. 8. Simulated electric field distribution of horn antenna (a) without lens (b) with proposed lens.

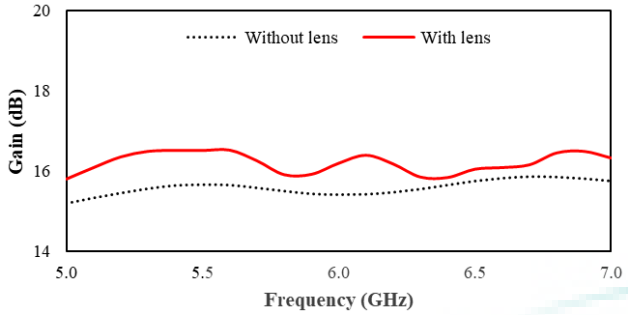

Fig. 9. Gain performance of horn antenna with and without lens.

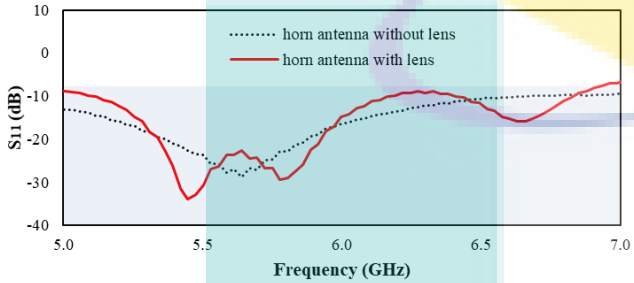

Fig. 10. Frequency dependency measured return loss of the horn antenna.

TABLE IV. THE MEASURED RADIATION CHARACTERISTIC OF THE HORN ANTENNA WITH AND WITHOUT LENS.

Frequency (GHz)	SLL (dB)		Beamwidth (Degrees)	
	Without lens	*With lens*	*With lens*	*Without lens*
5.0	-10	-7	22	28
5.5	-8	-17	18	26
5.9	-1	-7	24	50

V. CONCLUSION

The design of directive component for horn antenna in biomedical imaging system, using phase correction technique has been presented. A horn antenna with proposed flat lens is designed and simulated. The proposed lens is proved able to enhance the performance of horn antenna. As frequency increases, the directivity and SLL are increasing significantly, which is enough to be used for biomedical imaging system. The lens is able to convert the spherical waves from horn antenna to planar waves where the signal of horn antenna with proposed lens is more directive. The proposed flat lens provided several advantages, which are low-cost and easier to fabricate which can reduce the complexity compared to spherical shape used in classical Luneberg lens.

ACKNOWLEDGMENT

Authors would like to extend their gratitude to Universiti Malaysia Pahang and Ministry of Education (MOE) under Fundamental Research Grant Scheme (FRGS) with reference no. FRGS/1/2018/STG02/UMP/02/1 or RDU190140. This work also was partly supported by the Research and Innovation Department, Universiti Malaysia Pahang (grant no. RDU170370).

REFERENCES

[1] Hajisaeid, E., Dericioglu, A. F., and Akyurtlu, A. “All 3-D Printed Free-Space Setup for Microwave Dielectric Characterization of Materials” IEEE Transactions on Instrumentation and Measurement, 67(8), 1877-1886, 2018.

[2] Ahmed, H., Hyun, J., and Lee, J. R. “Development of scanning single port free space measurement setup for imaging reflection loss of microwave absorbing materials. Measurement”, 125, 114-122, 2018.

[3] I. Lau & M. Frank and K. Shi & F. Lurz, A. Talai, R. Weigel and A. Koelpin. “An Accurate Free Space Method for Material Characterization in W- Band Using Material Samples with Two Different Thicknesses”. 202-205. 10.23919/EuMC.2018.8541437.

[4] M. S. B. A. Karim, Y. Konishi, K. Harafuji and T. Kitazawa, "Determination of Complex Permittivities of Layered Materials Using Waveguide Measurements," in IEEE Transactions on Microwave Theory and Techniques, vol. 62, no. 9, pp. 2140-2148, Sept. 2014.

[5] M. S. B. A. Karim, N. Binti Abu Talip Yusof and T. Kitazawa “. Scattering analysis of rectangular cavity with input and output waveguides and its application to material characterization,” 2017 IEEE Asia Pacific Microwave Conference (APMC), Kuala Lumpur, pp. 588-591, 2017.

[6] N. Hasan, N. Hussain, A. A. M. Faudzi, S. Shaharum, N. Yusof, & N. Noordin, N. A. A. B. Hj Mohtadzar and M. S. A. Karim, “Cured epoxy resin dielectric characterization based on accurate waveguide technique.” AIP Conference Proceedings. 2129. 020080. 10.1063/1.5118088, 2019.

[7] M. Kinoshita, & H. Kinouchi, M. S. A. Karim, K. Wakino andT. Kitazawa, “A Method of Evaluating High-Permittivity and Lossy Materials Using a Cylindrical Cavity Based on Hybrid Electromagnetic Theory.” Japanese Journal of Applied Physics. 51. 09LF03. 10.7567/JJAP.51.09LF03, 2012.

[8] S. Akbar,A. S. M. Shah, A.Abdullah, N. Yusof,S. Khatun, S. Shaharum, Syamimi and M. S. A. Karim, “An Accurate Characterization of Different Water Properties Using Resonant Method for Underwater Communication Activity: Methods and Protocols.” , (2019).

[9] S. F. Hazali, N. Yusof, A. A. M. Faudzi, S. Khatun, S. Shaharum, Syamimi and M. S. A. Karim, “Design of Ultra-Wideband (UWB) Horn Antenna for Non-destructive Fruit Quality Monitoring.” In: Md Zain Z. et al. (eds) Proceedings of the 10th National Technical Seminar on Underwater System Technology 2018. Lecture Notes in Electrical Engineering, vol 538. Springer, Singapore.

[10] S. Zhang, R. K. Arya, S. Pandey, Y. Vardaxoglou, W. Whittow and R. Mittra, “3D-printed planar graded index lenses,” IET Microwaves, Antennas Propag., vol. 10, no. 13, pp. 1411–1419, 2016.

[11] C. A. Fernandes, E. B. Lima, and J. R. Costa.” Dielectric lens antennas”, Handb. Antenna Technol., vol. 2, pp. 1001–1064, 2016.

[12] S. Zhang, & J. Y. Vardaxoglou, W. Whittow, R. Mittra, “3D-printed flat lens for microwave applications.” 10.1109/LAPC.2015.7366130, 2015.

[13] R. M. Hashmi, B. A. Zeb and K. P. Esselle, "Wideband High-Gain EBG Resonator Antennas With Small Footprints and All-Dielectric Superstructures," in IEEE Transactions on Antennas and Propagation, vol. 62, no. 6, pp. 2970-2977, June 2014.

[14] J. Qiu, Y. Suo and W. Li, "Research and design on ultra-wideband dielectric hemispheric lens loaded quad-ridged horn antenna," 2007 6th International Conference on Antenna Theory and Techniques, Sevastopol, 2007, pp. 253-255, 2007.

[15] D. Wu, Z. Feng and X. Zhuang, "A novel focusing lens conical horn antenna loaded with dielectric," 2015 IEEE International Wireless Symposium (IWS 2015), Shenzhen, 2015, pp. 1-4, 2015.

[16] A. Patri and J. Mukherjee. “Fish-eye shaped dielectric flat lens design utilizing 3-D printing technology.” 2016 IEEE International Symposium on Antennas and Propagation (APSURSI), Fajardo, pp. 1843-1844, 2016.

[17] J. Tozawa, K. Morimoto, H. Deguchi and M. Tsuji, “Beam-tilted lens-corrected horn antennas for wide-angle radiation,” 2017 International Symposium on Antennas and Propagation (ISAP), Phuket, pp. 1-2, 2017.

[18] G. Boussatour, P. -. Cresson, B. Genestie, N. Joly and T. Lasri, "Dielectric Characterization of Polylactic Acid Substrate in the Frequency Band 0.5–67 GHz," in IEEE Microwave and Wireless Components Letters, vol. 28, no. 5, pp. 374-376, May 2018.

[19] Q. Wu, P. Pan, F. Y. Meng, L. W. Li, and J. Wu, “A novel flat lens horn antenna designed based on zero refraction principle of metamaterials,” Appl. Phys. A Mater. Sci. Process., vol. 87, no. 2, pp. 151–156, 2007.

[20] A. M. Abbosh, “Directive Antenna for Ultrawideband Medical Imaging Systems,” International Journal of Antennas and Propagation, vol. 2008, Article ID 854012, 6 pages, 2008.

[21] A. Karanth, N. Onkar, N. S. N. Smitha, Sridhara and V. Singh, "Through-wall imaging system using horn antennas," 2017 4th International Conference on Advanced Computing and Communication Systems (ICACCS), Coimbatore, 2017, pp. 1-6.

[22] M. K. T. Al-Nuaimi, W. Hong, and Y. Zhang, “Design of high-directivity compact-size conical horn lens antenna,” IEEE Antennas Wirel. Propag. Lett., vol. 13, pp. 467–470, 2014.